Journal of Medicinal Chemistry Article

J. Med. Chem. **2010,** *53,* 3465–3479 **3465**
DOI: 10.1021/jm901004c

Design, Synthesis, and Interaction Study of Quinazoline-2(1*H*)-thione Derivatives as Novel Potential Bcl-x_L Inhibitors

Yu Feng,[†,‡] Xiao Ding,[†,§] Tao Chen,[†,∥] Lili Chen,[‡] Fang Liu,[⊥] Xu Jia,[‡] Xiaomin Luo,[§] Xu Shen,[‡] Kaixian Chen,[§] Hualiang Jiang,[§] Hui Wang,*[,∥] Hong Liu,*[,§] and Dongxiang Liu*[,‡]

[‡]*Department of Molecular Pharmacology, and* [§]*Center for Drug Design and Discovery, Shanghai Institute of Materia Medica, Chinese Academy of Sciences, Shanghai 201203, China,* [∥]*Institute for Nutritional Sciences, Shanghai Institutes for Biological Sciences, Chinese Academy of Sciences, Graduate School of the Chinese Academy of Sciences, Shanghai 200031, China, and* [⊥]*School of Pharmaceutical Engineering, Shenyang Pharmaceutical University, Shenyang, Liaoning 110016, China.* [†]*Authors equally contributed to this work*

Received July 7, 2009

Development of inhibitors to antagonize the activities of antiapoptotic Bcl-2 family proteins is of particular interest in cancer chemotherapy. We discovered a quinazoline-2(1*H*)-thione derivative (DCBL55) as a new Bcl-x_L, Bcl-2, and Mcl-1 inhibitor by virtual database screening. We systematically modified the structure of compound **1** by chemical synthesis. The interactions of the compounds with Bcl-x_L were predicted by molecular modeling simulations, which were confirmed by structure−activity relationship analysis and protein mutation studies. Three locations at the hydrophobic groove of Bcl-x_L, referred to as P2, P4, and P5, were found to contribute to the ligand interactions. Although the compounds induced mitochondrial potential reduction, caspase activation, and ROS generation, the cytotoxicities and the ultrastructural changes of outer mitochondrial membrane suggested that the compounds may target additional proteins outside the Bcl-2 family. Altogether, the present study provides new lead compounds and critical structural information for further development of more potent and specific inhibitors of antiapoptotic Bcl-2 family proteins.

Introduction

Acute myeloid leukemia (AML)[a] is a heterogeneous group of malignant diseases arising from the progressive genetic damage in hemopoietic progenitor cells. Although the treatment strategies and supportive cares have been improved, the prognosis in old and in secondary AML patients remains poor.[1] The primary cause of the treatment failures in AML is the emergence of drug resistance and the early relapse, which is frequently due to the defects in the mitochondria-mediated apoptotic pathway.[1,2] This pathway is regulated by Bcl-2 family members including antiapoptotic proteins (e.g., Bcl-2, Bcl-x_L, Mcl-1) and proapoptotic proteins (e.g., Bax, Bad, Bid).[2] In particular, antiapoptotic proteins such as Bcl-x_L heterodimerize with proapoptotic proteins. Overexpression of antiapoptotic proteins can protect cancer cells from apoptosis.

Protein sequence analysis and structure−function studies revealed that the BH3 domain of proapoptotic proteins is the fundamental motif for dimerization with antiapoptotic proteins. The dimerization of Bcl-2 family proteins remained confusing until the first three-dimensional (3D) structure of a complex of Bcl-x_L with the Bak BH3 domain peptide was elucidated. The complex structure showed that the BH3 peptide is an amphipathic α-helix and binds to a hydrophobic groove on the surface of Bcl-x_L.[3] Based on these studies, mimicking the BH3 peptide with chemical compounds that bind to the same pocket became a drug discovery strategy to search for antiapoptotic protein inhibitors.

Beginning with the pioneering works of Wang et al.[4] and Degterev et al.,[5] more than a dozen of nonpeptidic Bcl-x_L or Bcl-2 inhibitors have been identified.[6,7] These compounds include HA14-1 (a chromene derivative, **14**), BH3I-1 (a thiazolidin derivative, **15**), and BH3I-2 (a benzenesulfonyl derivative, **16**), which bind to Bcl-2 or Bcl-x_L with an IC_{50} or K_i in the micromolar range (Figure 1). Another Bcl-x_L inhibitor, the indole derivative GX015-070[8] (obatoclax), has advanced into clinical trials for late-stage chronic lymphocytic leukemia. Gossypol,[9] a natural product extracted from cotton seeds and roots, was used to treat patients with metastatic adrenal cancer and breast cancer before it was recognized as a BH3 mimetic. It is now known that (−)-gossypol, the active enantiomer, binds to Bcl-2 family proteins (Bcl-2, Bcl-x_L, and Mcl-1) with good affinities[10] and has entered into clinical trials for advanced malignancies. Recently, ABT-737 (**17**) was reported as a potent nonpeptidic inhibitor with low nanomolar affinities to Bcl-2, Bcl-x_L, and Bcl-w but devoid of significant affinity to Mcl-1.[11]

Although numerous efforts have been focused on Bcl-2 family proteins in the last two decades and there is a strong need for effective drugs targeting antiapoptotic proteins, no Bcl-x_L or Bcl-2 inhibitor drug is yet available in the market due to problems such as structural stability, selectivity, and toxicity

*To whom correspondence should be addressed. Tel: +86-21-50806600. Fax: +86-21-50807088. E-mail: huiwang@sibs.ac.cn (H.W.); hliu@mail.shcnc.ac.cn (H.L.); dxl@mail.shcnc.ac.cn (D.L.).

[a] Abbreviations: AML, acute myeloid leukemia; BH domain, Bcl-2 homology domain; FITC, fluorescein isothiocyanate; SPR, surface plasmon resonance; FP, fluorescence polarization; SAR, structure−activity relationship; ROS, reactive oxygen species; JC-1, 5,5′,6,6′-tetrachloro-1,1′,3,3′-tetraethylbenzimidazolylcarbocyanine iodide; DCFH-DA, 2′,7′-dichlorofluorescin diacetate.

Published on Web 04/20/2010

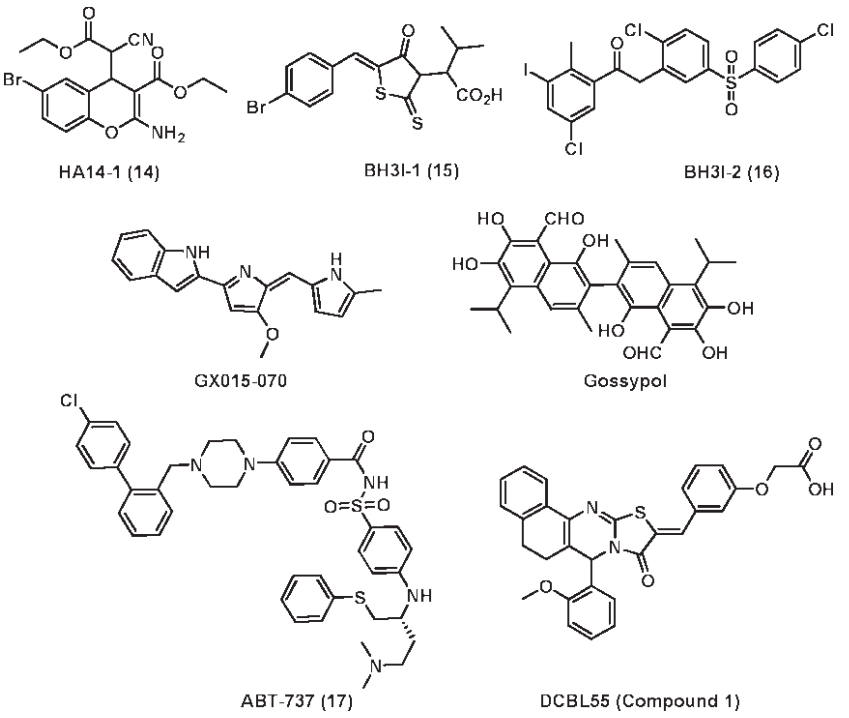

Figure 1. Chemical structures of several Bcl-x_L/Bcl-2 small molecule inhibitors.

of the inhibitors. Therefore, it is still a great challenge to discover and develop novel efficient Bcl-x_L inhibitors, without disadvantages of the former inhibitors. In this study, we discovered a quinazoline-2(1*H*)-thione derivative (DCBL55, **1**, Figure 1) as a Bcl-x_L inhibitor with IC_{50} of 3.4 μM by virtual database screening. We systematically modified the structure of compound **1** by chemical synthesis and studied the structure−activity relationship (SAR). The orientations of the compounds in the hydrophobic groove of Bcl-x_L were predicted by molecular docking and molecular dynamics (MD) simulations, which were then confirmed by protein mutation study, SAR of the compounds, and the *in vitro* binding assay of compound **1** enantiomers with Bcl-x_L. Three locations at the hydrophobic groove of Bcl-x_L, referred to as P2, P4, and P5, were found to contribute to the ligand interactions. Further, we evaluated the selectivity of the compounds among antiapoptotic Bcl-2 family proteins. Though the compounds bind to Bcl-2, Bcl-x_L, and Mcl-1, they exhibited a similar affinity to Bcl-2 and Bcl-x_L but a relatively weaker affinity to Mcl-1. Altogether, the present study provides new lead compounds and important structural information for future development of more potent and specific inhibitors of antiapoptotic proteins.

Materials and Methods

Molecular Modeling. (A) Virtual Screening of Chemical Compound Database. The coordinates of Bcl-x_L were extracted from its complex crystal structure with **17** (PDB code: 2YXJ). Chemical potential and charges were assigned to the residues with CVFF force field. The protein structure without water was minimized with 500 steps of steep descent optimization and 10000 steps of conjugate gradient optimization until the maximum energy derivative is less than 0.05 kcal/Å in Discover (version 2.98) (Accelrys Software Inc.). The main-chain atoms were tethered during the structure minimization. Spheres were generated by AutoMS and sphgen to describe the shape of the hydrophobic groove in Bcl-xL, which is near the residues of Glu96, Phe97, Arg100, Tyr101, Ala104, Phe105, Leu108, Val126, Glu129, Leu130, Asn136, Arg139, Val141, Ala142, Phe146, Phe191, and Tyr195. The hydrophobicity and electrostatic properties at the grid points surrounding the hydrophobic groove were calculated by the program of Grid. Chemical compounds from the SPECS database (http://www.specs.net) were placed into the pocket individually, the conformation and orientation of which were optimized with a single anchor search and torsion minimization method by using a parallelized Dock 4.0 program on a PC cluster (http://dock.combio.ucsf.edu). The configuration of the compound in the pocket was further optimized with 100 steps of steep descent minimization and then evaluated with the energy score function in Dock 4.0. The interactions of the top 2000 chemical compounds with Bcl-x_L, ranked out by virtual database screening, were visually verified by chemists, mainly focusing on steric bump, hydrogen bond, and hydrophobic interactions between the compounds and Bcl-x_L residues. Finally, 77 compounds were purchased and subjected to the binding assay with surface plasmon resonance (SPR) technology.

(B) Interaction Study of the Compounds with Bcl-x_L by Docking and MD Simulations. Chemical structures of compounds **1**, **12h**, and **13** were built with the sketch molecule module in Sybyl 7.3 (Tripos). The atoms were assigned with Gasteiger−Huckel charges. The structures were optimized with 100 steps of Powell minimization and 10000 steps of conjugated gradient minimization until the energy derivation is less than 0.05 kcal/(mol·Å). There are a chiral carbon at C-7 and a C=C bond that may adopt *cis* or *trans* conformation at the structural scaffold of the compounds (Table 1). Thus, four isomeric forms for each compound were generated and docked into the hydrophobic groove with the FlexX Single Receptor (RDF) module in Sybyl. Compound **17** in its complex structure of Bcl-x_L (PDB code: 2YXJ) was used as the reference for docking. All of the

Table 1. Chemical Structures of the Compounds and Their Bcl-x_L Inhibitory Activities

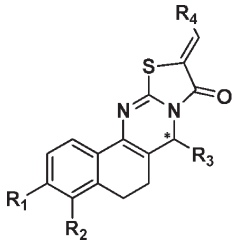

Compound	R_1	R_2	R_3	R_4	IC_{50} (μM)
1	H	H		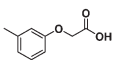	3.4±0.8
6	H	H		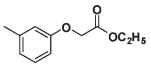	>100
7	H	H		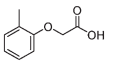	12.1±3.1
8	H	H		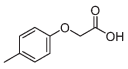	36.0±8.3
9	H	H		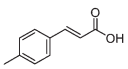	12.7±1.7
10	H	H		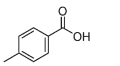	12.6±2.6
11	H	H		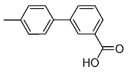	26.7±16.5
12	H	H		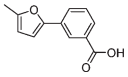	5.3±0.6
13	H	H		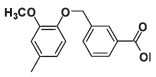	17.4±5.0
1a	H	H		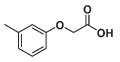	10.3±2.2
1b	H	H		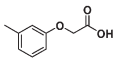	5.4±1.5
1c	H	H		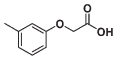	19.7±4.8
1d	H	H		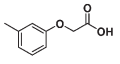	40.4±8.8
1e	H	OCH_3		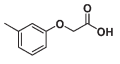	>100
1f		H		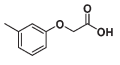	>100
1g		H		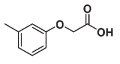	>100
1h	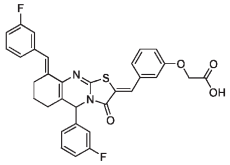				>100
1i	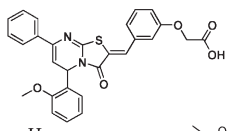				72.0±26.1
12a	H	H		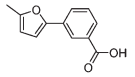	12.6±5.4
12b	H	H			6.2±0.6
12c	H	H			3.0±1.0
12d	H	H			5.2±1.7
12e	H	H			1.9±0.6
12f	H	H			13.4±2.5
12g	H	H			35.9±13.7
12h	H	H			6.9±0.8
12i	H	H			7.3±3.0
12j	H	OCH_3			>100
12k					>100
15					6.2±0.5

parameters were set as the default except the maximum number of poses per ligand was 500. The orientation for the most favorable isomeric form of each compound was determined. The complex structures of Bcl-x_L with compounds **1**, **12h**, and **13** were further optimized in Insight II 2000. In detail, Bcl-x_L residues were added with hydrogen with the capping mode off. The potentials for Bcl-x_L residues and the atoms of the compounds were fixed with the CVFF force field. The

complex structures were optimized with 1000 steps of steep descent minimization and 6000 steps of conjugate gradient minimization until the energy derivation is less than 0.05 kcal/Å, during which the main-chain atoms of Bcl-x_L were fixed and the distances between several atoms of the compounds and the C_α atoms of Bcl-x_L residues were restrained in the range of 3.0−7.5 Å in case of any dissociation event of the compounds from the hydrophobic groove. Then, the complex structures were further optimized with 100 iterations of MD simulations in Discover (version 2.98). Specifically, 1000 steps of MD simulations were initialized at the temperature of 300 K, followed by 2000 steps of simulations at 600 and 300 K, respectively. The archived complex structures for each compound were optimized with 1000 steps of steep descent minimization and 10000 steps of conjugate gradient minimization until the energy derivation is less than 0.05 kcal/Å. At this stage, the constraints were released, and the atoms were free to move during the minimization. On the basis of the structure−activity relationship study (Table 1), the most reasonable interaction model for compounds **1**, **12h**, and **13** was determined out of the 100 optimized archive structures.

Biological Assay. (A) *In Vitro* Binding Assay by SPR. The binding affinity of compounds with Bcl-x_L or its mutant proteins was assayed using a surface plasmon resonance based biosensor instrument Biacore 3000 (Biacore AB, Uppsala, Sweden). The flow cell of the CM5 sensor chip (catalog no. BR-1000-14; Biacore AB) was activated by injecting a fresh mixture of equal volume of 0.2 M *N*-ethyl-*N*′-dimethylaminopropylcarbodiimide and 50 mM *N*-hydroxysuccinimide at 25 °C for 7 min. The protein stock solution was diluted with 10 mM sodium acetate buffer (pH 4.7) to 1 mg/mL and immobilized to the surface of the sensor chip. Excessive carboxyl groups were blocked by injecting 1 M ethanolamine hydrochloride at pH 8.5 for 7 min. Equilibration of the system was completed by continuous flow of HBS-EP buffer (10 mM HEPES, 150 mM NaCl, 3 mM EDTA, and 0.005% (v/v) P20, pH 7.4) through the sensor chip overnight. For the screening assay, 10 mM stock solutions of compounds in DMSO were diluted in HBS-EP buffer to 10 μM and flowed through the sensor chip at a speed of 30 μL/min. To determine the affinity of compounds with Bcl-x_L or its mutant proteins, gradient concentrations of compounds were injected into the channel at a flow rate of 30 μL/min for 60 s, followed by disassociation for 120 s. The kinetic parameters of the interaction were determined by the 1:1 Langmuir binding fitting model using BIAevaluation software (version 3.2).

(B) Fluorescence Polarization (FP) Assay. Bid BH3 domain peptide (sequence: EDIIRNIARHLAQVGDSMDR) was synthesized and labeled with fluorescein isothiocyanate (FITC) at the N-terminus. For the competitive binding assay, 200 nM Bcl-x_L, Bcl-2, or Mcl-1 was mixed with various concentrations of compounds in phosphate-buffered saline buffer (PBS, pH 7.4). After 1 h of incubation at 25 °C, an equal volume of 200 nM FITC labeled BH3 peptide was added. After 10 min of incubation at 25 °C, the fluorescence polarization was measured on a POLARstar OPTIMA microplate reader (BMG LABTECH, Germany). The excitation wavelength and emission wavelength were set to 485 and 520 nm, respectively.

(C) Cytotoxicity Assay. The cytotoxic activities against human cancer cells were studied by the MTT colorimetric assay. A2780, OVCAR-3, HepG2, BEL-7404, PC-3, and K562 cells were obtained from the American Type Culture Collection (Manassas, VA). All cell culture supplies were obtained from Invitrogen (Carlsbad, CA). Thiazolyl blue tetrazolium bromide (catalog no. M5655) and dimethyl sulfoxide (catalog no. D5879) were purchased from Sigma-Aldrich (St. Louis, MO). Cells were cultured in RPMI 1640 (A2780, OVCAR-3, PC-3, and K562) or DMEM (HepG2 and BEL-7404) and maintained in a Thermo incubator (Waltham, MA) with a humidified air containing 5% CO_2 at 37 °C. All culture media contained 10% FBS and 1% penicillin−streptomycin. Four-thousand cells (per well) were seeded in 96-well plates and treated with the compounds for 48 h at serial concentrations. Then 10 μL of MTT solution (5 mg/mL in PBS) was added to each well. Plates were incubated for an additional 2−4 h at 37 °C. The supernatant was carefully removed, and 100 μL of DMSO was added to dissolve the formazan crystals. The absorbance at 570 nm was recorded on a SpectraMax 190 microplate reader (Molecular Devices) and used to calculate the cell survival percentage and EC_{50}, accordingly.

Scheme 1[a]

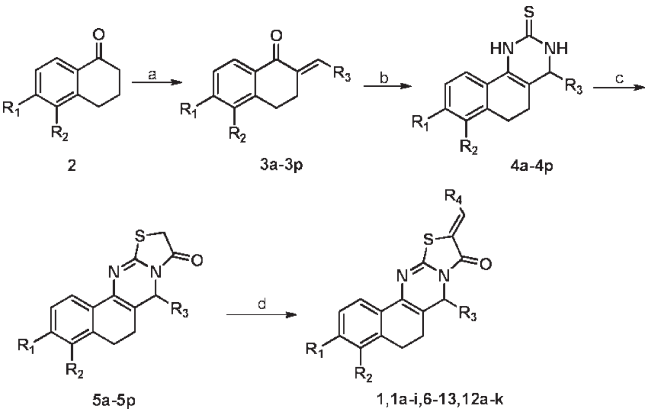

[a] Reagents and conditions: (a) R_3CHO, KOH, EtOH, room temperature, 4 h; (b) NH_2CSNH_2, KOH, EtOH, reflux, 5 h; (c) $ClCH_2COOH$, NaOAc, HOAc, Ac_2O, reflux, 2 h; (d) R_4CHO, piperidine, EtOH, reflux, overnight.

Chemistry. (A) Structural Analogue Design of Compound 1. Based on the structural feature of compound **1,** 28 new analogues (Table 1, compounds **1a**−**1i**, **6**−**13**, and **12a**−**12k**) were designed and synthesized. First, we kept the 2-methoxybenzyl group of compound **1** and replaced the 2-(3-phenoxy)-acetic acid group with other types of benzoic acid groups or heteroaryl acid groups to get compounds **6**−**13**. The FP assay results showed that compounds **1** and **12** are the most active compounds, suggesting that the 2-(3-phenoxy)acetic acid group and 3-(5-furan-2-yl)benzoic acid group at R_4 are the most appropriate fragments for interaction with Bcl-x_L. Then, we kept the 2-(3-phenoxy)acetic acid group and changed the 2-methoxybenzyl group into a naphthalene or furan ring or introduced various substituent groups of R_1, R_2, and R_3 at the phenyl rings to obtain compounds **1a**−**1i**. Keeping the 3-(5-furan-2-yl)benzoic acid group of compound **12**, we obtained compounds **12a**−**12k** by changing the 2-methoxybenzyl group into other types of rings at R_3.

(B) Chemistry Synthesis Procedure. Compounds **1**, **1a**−**1i**, **6**−**13**, and **12a**−**12k** were synthesized through the route outlined in Scheme 1. Treatment of **2** with various aldehydes in ethanolic potassium hydroxide solution at room temperature quickly afforded 1-tetralones **3a**−**3p** with good yields.

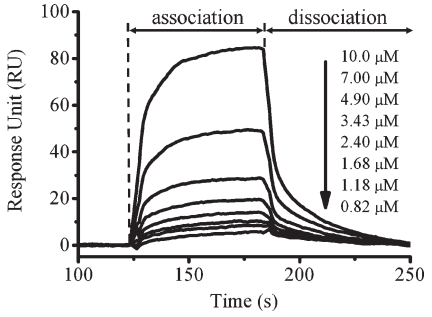

Figure 2. The response curve of the interaction between compound **1** and Bcl-x_L immobilized on a CM5 sensor chip by SPR.

3a−**3p** were converted to **4a**−**4p** by refluxing with thiourea in ethanolic potassium hydroxide solution. **4a**−**4p** were condensed with chloroacetic acid and anhydrous sodium acetate in glacial acetic acid and acetic anhydride to produce **5a**−**5p**, which were subsequently reacted with various aldehydes, respectively, in the presence of piperidine in ethanol, affording the target compounds **1**, **1a**−**1i**, **6**−**13**, and **12a**−**12k**. The details of the synthetic procedures and structural characterizations of the compounds are described in Experimental Section. The purities of the compounds are listed in Table S1 in Supporting Information.

Results and Discussion

Discovery of the Active Compound. The primary approach that we used to discover the Bcl-x_L inhibitor was virtual database screening. A total of 77 compounds were selected with Dock 4.0 from SPECS chemical compound database by targeting the hydrophobic groove of Bcl-x_L. To identify the active compound, we assayed the Bcl-x_L binding affinity of the 77 compounds with surface plasmon resonance technology. Bcl-x_L was first immobilized on the CM5 sensor chip. If a compound binds to the immobilized Bcl-x_L, the specific interaction that occurred on the chip can be detected by the change of the resonance. Among the 77 compounds, we found compound **1** brought about a concentration-dependent resonance change when flowing through the sensor chip at serial concentrations (Figure 2). The data of the response curve were fitted to a 1:1 interaction model (i.e., A + B = AB) by using the software BIAevaluation (BIAcore AB).[12] The kinetic parameters of the interaction between Bcl-x_L and compound **1** were calculated. The association rate k_a, the dissociation rate k_d, and the equilibrium dissociation constant K_D are 1.05×10^3 M^{-1} s^{-1}, 9.98×10^{-3} s^{-1}, and 9.50×10^{-6} M, respectively.

Since the compound is designed to target the BH3 peptide binding pocket in Bcl-x_L, compound **1** should compete with BH3 peptide to bind Bcl-x_L. To confirm the presumption, we measured the affinity of the compound to Bcl-x_L by a competitive binding assay based on fluorescence polarization. In this assay, FITC was coupled to the N-terminus of a peptide derived from the BH3 domain of Bid, which has been shown to bind to Bcl-x_L, Bcl-2, and Mcl-1 with high affinities.[7] When the FITC-labeled Bid BH3 peptide binds to antiapoptotic Bcl-2 family proteins, the system has a high value of fluorescence polarization. After the addition of competitors, the FITC-labeled Bid BH3 peptide loses the contact with the proteins, and the value of fluorescence polarization decreases. As determined in our assay (Figure 3A), the IC_{50} of compound **1** is 3.4 μM, indicating

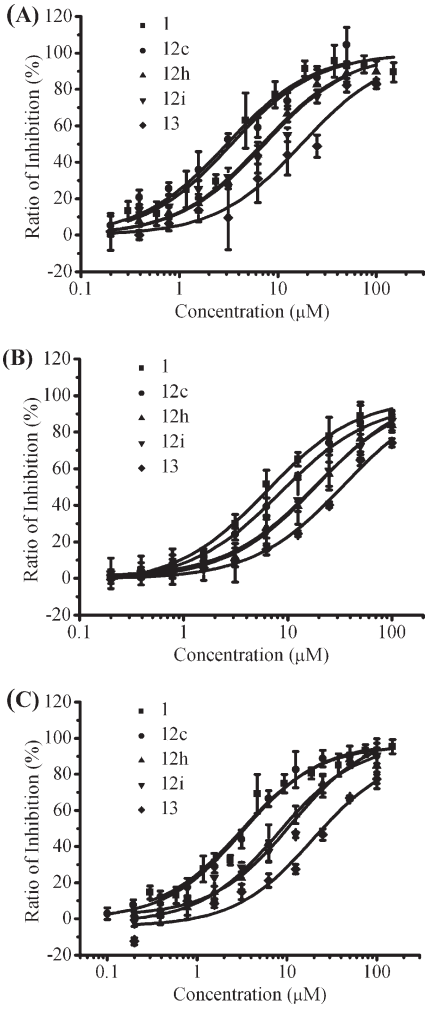

Figure 3. The inhibitory activities of compound **1** and its analogues (**12c**, **12h**, **12i**, and **13**) to Bcl-x_L, Bcl-2, and Mcl-1 by a competitive binding assay based on fluorescence polarization. The substrate for the assay was a FITC-labeled Bid BH3 domain peptide (amino acid sequence: EDIIRNIARHLAQVGDSMDR). (A−C) The inhibitory activities of the compounds to Bcl-x_L, Mcl-1, and Bcl-2, respectively.

that compound **1** indeed binds to the hydrophobic groove of Bcl-x_L and has a better affinity to Bcl-x_L than compound **15** (Table 1).[7]

So far, there have been six human antiapoptotic Bcl-2 family proteins identified. Some of them such as Bcl-2, Bcl-x_L, and Mcl-1 seem to contribute to the drug resistance in cancer cells.[6] Inhibition of multiple antiapoptotic Bcl-2 family proteins may be necessary to achieve optimal therapeutic effect.[13] One approach to enhance the therapeutic effect would be the combinational usage of inhibitors that specifically target different antiapoptotic proteins. Alternatively, a broad-spectrum or semiselective antagonist that inhibits all or a subset of six antiapoptotic proteins may be used. To evaluate the inhibitory potency of the compounds targeting other antiapoptotic proteins, we measured the binding affinity of compound **1** and its analogues to Bcl-2 and Mcl-1. As shown in Figure 3 and Table 2, compound **1** binds to Bcl-2 and Bcl-x_L with comparable affinities, while the affinity to Mcl-1 was 6.4 μM, which is about 2-fold worse than that of Bcl-2 and Bcl-x_L. Similarly, the binding affinities of analogues **12c**, **12h**, **12i**, and **13** to Mcl-1 were about 1.7−2.8-fold less effective than their affinities to Bcl-2 and Bcl-x_L, respectively. The micromolar

binding affinities of compounds **1** and **12c** to Bcl-2, Bcl-x_L, and Mcl-1 demonstrated that the designed inhibitors are antagonists for multiple antiapoptotic Bcl-2 family proteins and therefore may be used as the lead compounds for further structural refinement and pharmacological studies in leukemia as well as other types of cancers.

Structure−Activity Relationship. According to the FP assay, 22 of the synthesized analogues (**1**, **1a**−**1d**, **1i**, **7**−**13**, and **12a**−**12i**) showed a Bcl-x_L inhibitory activity with an IC_{50} of 1.9−72.0 μM (Table 1). Structurally, all of the compounds except **1h**, **1i**, and **12k** have the same chemical scaffold. The assay results indicated that **1**, **12c**, and **12e** are the most active compounds, suggesting that the 2-(3-phenoxy)-acetic acid group and 3-(5-furan-2-yl)benzoic acid group are the optimal fragments at the R_4 position. The activity disappeared when the carboxy group of R_4 was acetylated (comparing **1** and **6**). While changing the carbonyl group from the *meta* position into *ortho* (**7**) or *para* position (**8**), the IC_{50} was reduced to 12.1 and 36.0 μM, respectively.

Table 2. Binding Affinity of Compound **1** and Its Analogues with Bcl-x_L, Mcl-1, and Bcl-2 Determined by Fluorescence Polarization Assay (IC_{50}, μM)

compd	Bcl-x_L	Mcl-1	Bcl-2
1	3.4 ± 0.8	6.4 ± 0.8	3.1 ± 0.9
12c	3.0 ± 1.0	8.6 ± 1.2	3.2 ± 0.4
12h	6.9 ± 0.8	18.6 ± 3.4	8.0 ± 1.0
12i	7.3 ± 3.0	19.2 ± 2.9	11.1 ± 2.9
13	17.4 ± 5.0	34.4 ± 8.5	19.4 ± 7.8

However, the activity was again recovered to 12.7 and 12.6 μM, respectively, when replacing the 2-(3-phenoxy)acetic acid group with the cinnamic acid group (**9**) or benzoic acid group (**10**), which indicated that decreasing the length or increasing the rigidity of the carbonyl chain may be in favor for the binding activity. Besides, replacing the 2-(3-phenoxy)acetic acid group with biphenyl-3-carboxylic acid (**11**) or 3-((2-methoxyphenoxy)methyl)benzoic acid (**13**) reduced the IC_{50} to 26.7 and 17.4 μM, respectively. Introducing different substitutions (such as methoxy (**1e**, **12j**), benzyloxy (**1f**), and 2-(biphenylcarbonyloxy)phenoxy (**1g**)) to R_1 and R_2 also abolished the activities. Meanwhile, the activity disappeared or was reduced significantly when ring A or B was replaced with other groups (**1 h**, **1i**, and **12k**). Substitution of the R_3 group also affects the activity. It was shown that introducing substituents to the benzene ring of R_3 may increase the activity compared to the nonsubstituent benzene group (**1a** and **1b**, **12a** and **12b**−**12e**). Compounds with the *meta* substituents of the R_3 groups are more potent than the *ortho*- and *para*-substituents (**12c** > **12b**, **12d**). In addition, substitution of the benzyl group with the smaller furan group (**1d**, **12g**) reduced the IC_{50} to 40.4 μM and > 100 μM, while replacing with bigger naphthyl group (**1c**, **12f**) also reduced the IC_{50} to 19.7 and 13.4 μM, respectively.

Binding Site and Interaction Models of the Compounds with Bcl-x_L. To map the binding site of compound **1** and its analogues, we built the complex structures of the compounds with Bcl-x_L by docking and molecular dynamics simulations. The complex structures of the compounds showed that

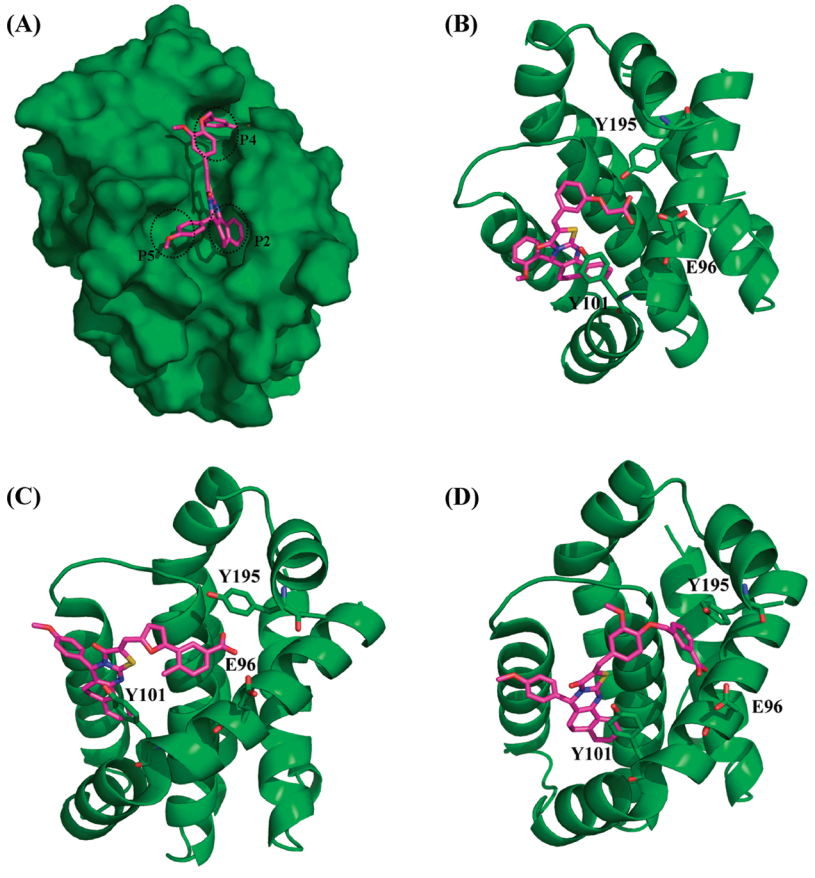

Figure 4. The interaction models of compounds **1**, **12h**, and **13** with Bcl-x_L. (A) The binding site and orientation of the compounds (represented by compound **13**) in the hydrophobic groove of Bcl-x_L. The protein is rendered in green, while the compound is rendered in red. The binding pockets P2, P4, and P5 are labeled with dash circles. (B−D) The binding model of compounds **1** (B), **12h** (C), and **13** (D) in complex with Bcl-x_L. Bcl-x_L is rendered as a cartoon, while the residues of Glu96, Tyr101, and Tyr195 and the compounds are rendered as sticks.

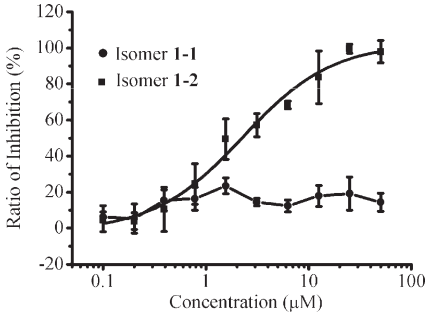

Figure 5. The binding affinities of compound **1** enantiomers to Bcl-x_L by FP assay.

compound **1** (Figure 4B) bound to the hydrophobic groove of Bcl-x_L with *R* isomeric form at the C-7 chiral carbon, while compound **12h** (Figure 4C) and compound **13** (Figure 4D) bound with *S* forms. To validate the interaction models, we separated the enantiomers of compound **1** by chiral chromatography (Supporting Information Figure S1). The FP assay showed that isomer **1-2** (*R*) bound to Bcl-x_L with the IC_{50} of 1.9 μM, while isomer **1-1** (*S*) did not bind to the protein (Figure 5). This result is in agreement with the complex structure models, which strongly supports the rationality of the interactions of the compounds with Bcl-x_L predicted by our molecular modeling simulations.

According to the complex structures, three locations at the hydrophobic groove (i.e., P2, P4, and P5) of Bcl-x_L should have critical interactions with the compounds. The binding pocket P2 is the same as that of **17**, which is formed by residues Tyr101, Ala104, Leu108, Val126, Asn135, Ala142, and Ser145. The pocket P4 is formed by residues Glu96, Phe97, Gly138, and Tyr195, while the pocket P5 is formed by residues Leu130, Arg132, and Arg139.

To verify the binding site of the compounds, we introduced a series of point mutations at the Bcl-x_L hydrophobic groove based on the complex structure models. Specifically, the residue of Glu96, Tyr101, or Tyr195 was substituted with alanine. Bcl-x_L mutant proteins were expressed in *Escherichia coli* and purified with glutathione Sepharose resin. The circular dichroism and BH3 peptide binding assay implicated that the mutants were well folded and had an intact binding pocket (Supporting Information Figure S2). To assess the effect of the mutations on the binding affinity of the compounds, gradient concentrations of compound **1**, **13**, or **12h** were flowed through the CM5 sensor chip that was immobilized with wild-type or mutant Bcl-x_L proteins. The binding affinity of compound **1** with E96A or Y195A, characterized by the dissociation constant (K_D), was reduced 4-fold and 95-fold relative to wild-type Bcl-x_L (Table 3). The binding affinity of compound **12h** with E96A or Y101A was reduced over 3-fold and 10-fold, while the binding affinity of compound **13** with E96A, Y101A, or Y195A was reduced over 25-, 25-, and 17-fold, respectively. Clearly, the SPR assay demonstrated that the residues of Glu96, Tyr101, and Tyr195 contributed significantly to the interaction of Bcl-x_L with compound **1** and its analogues. As Tyr101 is at the P2 pocket while Glu96 and Tyr195 are at the P4 pocket, the effects of these mutations demonstrated that these pockets are involved in the interactions with the compounds.

To further validate the interaction models, we correlated the SAR of the compounds with their interactions with Bcl-x_L. According to the models, the R_4 group of the compounds

Table 3. Binding Affinity of Bcl-x_L and Its Mutant Proteins with Compound **1** and Its Analogues Determined by SPR Assay (K_D, μM)

proteins	compd **1**	compd **12h**	compd **13**
WT	9.50	96.3	38.5
E96A	34.8	296	> 1000
Y101A	6.94	> 1000	> 1000
Y195A	904	60.1	682

binds to the P4 pocket through hydrogen bond and hydrophobic interactions (Figure 4). Of the 29 synthesized analogues, compounds **1**, **12c**, and **12e** are the most active compounds, suggesting that the 2-(3-phenoxy)acetic acid group and 3-(5-furan-2-yl)benzoic acid group are the most appropriate fragments for the interactions. The binding model of compound **1** (Figure 4B) showed that the residues of Glu96 and Tyr195 form hydrogen bonds with the carboxyl on R_4 of compound **1**, which was consistent with the decreased affinities of the compound with the mutant protein of E96A or Y195A (Table 3). For the same reason, the activity of the compound was abolished when the carboxy group of R_4 was acetylated (compound **6**). Changing the carbonyl group from the *meta* to *ortho* (**7**) or *para* position (**8**), the IC_{50} of the compounds was reduced to 12.1 and 36.0 μM, respectively. On the other hand, modifying the planarity or length of the R_4 fragment also affected the binding activity (comparing compounds **8** and **9**, or **10**). Different from compounds **1**−**10**, compounds **1i**, **12**, and **13** bind to the P4 pocket not only through hydrogen bond interaction but also through hydrophobic interaction to some extent. The complex structure model of compound **12h** with Bcl-x_L (Figure 4C) showed that the residue of Glu96 forms a hydrogen bond with the carboxyl on R_4, while the residue Tyr195 has no hydrophobic interaction or hydrogen bonding with R_4, which is consistent with the mutation results of E96A or Y195A by SPR assay (Table 3). When replacing the 3-(5-furan-2-yl)benzoic acid group with 3-((2-methoxyphenoxy)methyl)benzoic acid (compound **13**), the IC_{50} was reduced to 17.4 μM. The binding model of compound **13** with Bcl-x_L (Figure 4D) showed that the residue Glu96 forms a hydrogen bond with the carboxyl on R_4, while the residue Tyr195 has hydrophobic interaction with the phenyl group on R_4.

Besides, the complex structures indicated that the ring A of the compounds binds to the P2 pocket through hydrophobic interactions. The benzene ring is located deeply in the pocket. Little space was left between the benzene ring and the residues. This is the reason why the binding activity was decreased dramatically when different substitutions were introduced to R_1 and R_2 (compounds **1e**−**1g**). Meanwhile, replacing the ring A or B with other groups (**1 h**, **1i**, and **12k**) also abolished or significantly reduced the binding activity, due to the disruption of the hydrophobic interaction by the steric bump between the residues and the compound groups.

As to the P5 pocket, the R_3 groups of the active compounds have hydrophobic interactions with the side chains of Leu130, Arg139, and Arg132 based on the complex structure models (Figure 4). The SAR study showed that substitution at the benzene ring of R_3 could increase the activity compared to nonsubstituted benzene group (compare compounds **12a** and **12b**−**12e**). Compounds with substituents at the *meta* position of the R_3 groups are more potent than those with substituents at *ortho* and *para* positions (**12c** > **12b**, **12d**). While replacing the benzyl group with the smaller furan group (compounds **1d**, **12g**), the IC_{50} was reduced to 40.4 and 35.9 μM, respectively. This is because the furan ring is less hydrophobic when compared with the

Table 4. Cytotoxicity of Compound **1** and Its Analogues Assessed via MTT Assay (EC_{50}, μM)

	ovarian cancer		liver cancer		prostate cancer	leukemia
compd	A2780	OVCAR-3	HepG2	BEL-7404	PC-3	K562
1	4.57	1.54	12.7	7.9	37.65	50.87
6	17.81	47.50	32.3	92.3	45.03	> 100
7	7.81	4.44	41.9	9.5	ND	7.99
8	6.13	2.85	15.3	6.1	11.09	5.62
9	7.85	3.29	49.8	11.2	17.28	> 100
10	7.94	3.35	45	9.7	63.45	16.13
11	2.23	7.17	7.2	4.5	67.09	9.41
12	4.94	9.06	35.6	139.6	23.22	20.83
13	3.03	11.73	9.9	7.2	> 100	6.42
1a	5.49	2.73	14.5	7.8	> 100	7.04
1b	16.85	2.80	185.7	50.9	> 100	> 100
1c	7.52	2.21	19.9	3.1	67.98	6.33
1d	15.29	8.50	72.8	14	10.23	> 100
1e	6.95	27.76	47	46.5	> 100	> 100
1f	6.86	6.44	20.5	208.8	> 100	7.91
1g	2.16	6.80	78.2	54.4	16.62	6.82
1h	6.80	3.27	15.9	4.3	11.97	> 100
1i	9.98	22.24	175	> 500	65.25	> 100
12a	7.46	18.95	13.6	71.7	> 100	> 100
12b	> 100	76.60	> 500	> 500	31.23	> 100
12c	5.81	12.02	15.4	51.3	> 100	> 100
12d	7.38	5.85	35.10	25.89	13.41	26.26
12e	3.90	26.91	13.4	65.1	44.89	17.33
12f	6.34	18.68	> 500	203.7	24.24	22.94
12g	15.77	> 100	> 500	> 500	79.48	> 100
12h	13.08	7.21	> 100	24.65	12.03	72.32
12i	13.79	7.91	> 100	> 100	29.52	> 100
12j	4.52	7.84	10.7	4.8	35.16	65.16
12k	5.36	11.70	8	3.8	51.43	> 100

benzene ring. On the other hand, replacing the benzyl group with the bigger naphthyl group (compounds **1c**, **12f**), the IC_{50} was 19.7 and 13.4 μM, respectively, worse than that of compounds **1b** and **12c**, indicating that large rings like naphthalene may have a negative effect on the hydrophobic interactions.

Despite the extra contribution of the P5 pocket, the binding affinities of compound **1** and its analogues are weaker than that of **17**. The difference between the scaffolds of compounds **1** and **17** may account for the compromised binding affinity and selectivity. In the complex structure of **17**, the chlorobiphenyl group and thiophenyl group project deeply into the P2 and P4 pockets, respectively. Although the ring A of compound **1** overlays with the chlorobiphenyl group of **17**, the rigidity of rings A, B, and C of compound **1** restricts ring A from the optimal conformation. Similarly, the linker of **17** is longer than that in compound **1**, which renders flexibility of the thiophenyl group. Therefore, the thiophenyl group fits into the P4 pocket better than the R_4 group.

Compounds Induced Potent Cytotoxicity to Cancer Cells. Bcl-x_L, Bcl-2, and Mcl-1 are overexpressed in multiple cancer cells and contribute to their drug resistance to chemotherapy. Since compound **1** and its analogues bind to Bcl-x_L, Bcl-2, and Mcl-1 and inhibit their interactions with the BH3 domain of proapoptotic protein, it is reasonable to investigate their possible effect on cancer cells. The cytotoxicities of compound **1** and its analogues were evaluated with diverse cancer cell lines. Remarkably, most compounds induced a dose-dependent reduction in cell viability (Table 4). Compound **1** and its analogues exhibited cytotoxic potency against ovarian cancer cells (A2780, OVCAR-3), liver cancer cells (HepG2, BEL-7404), prostate cancer cells (PC-3), and leukemia cancer cells (K562).

Though *in vitro* assays have proven that compound **1** and its analogues bind to antiapoptotic Bcl-2 family proteins, the cytotoxicities of these compounds appeared not related to their *in vitro* binding affinities (Tables 1 and 4). For example, compounds **6**, **1e**, **1f**, **1g**, **1h**, **12j**, and **12k** which hardly bind to Bcl-x_L can induce the death of multiple cell lines. One possible explanation is that these compounds may not be selective Bcl-2 family inhibitors and thus do not exert their function exclusively through the Bcl-x_L pathway. As Vogler et al. reported, only **17** exerted its proapoptotic effect through Bax/Bak, while other Bcl-2 or Bcl-x_L inhibitors (obatoclax, gossypol, apogossypol, EM20-25, and chelerythrine) targeted additional proteins outside the Bcl-2 family.[14] With transmission electron microscopy, they found that exposure of chronic lymphocytic leukemia (CLL) cells to **17** induced mitochondrial swelling and discontinuities in the outer mitochondrial membrane. However, the outer mitochondrial membrane was intact in the case of obatoclax, gossypol, and apogossypol. In our experiments, K562 cells treated with compound **1** showed morphology characteristic of apoptosis such as chromatin condensation (Figure S3 in Supporting Information, black arrow). Meanwhile, the outer mitochondrial membrane remained intact, and the inner mitochondrial membrane was contracted (white arrow). The change of outer mitochondrial membrane suggests that compound **1** induced cell death not solely through Bcl-2 family proteins and may target additional proteins besides the Bcl-2 family.

Reduction of Mitochondrial Membrane Potential ($\Delta\Psi$m). Loss of mitochondrial membrane potential is an early event associated with apoptosis.[15] As shown in Supporting Information Figure S3, the mitochondrial morphology had been changed after the treatment of compound **1**. Therefore, it is reasonable to investigate whether compound **1** can induce

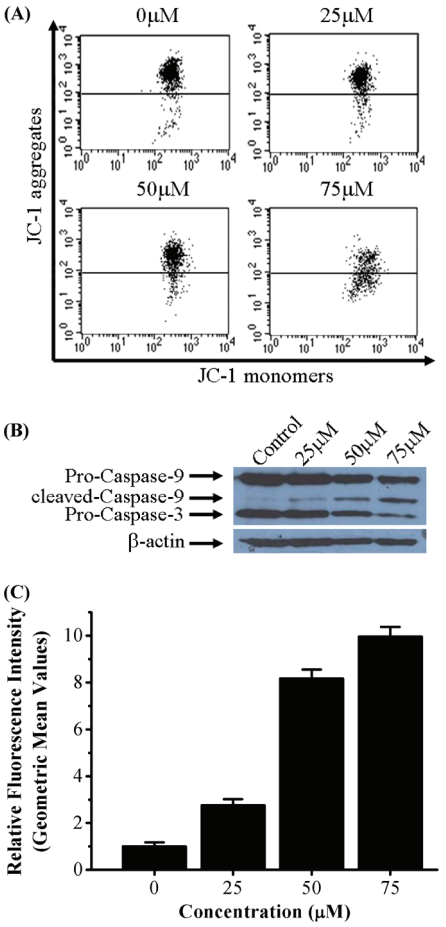

Figure 6. (A) Assessment of mitochondrial membrane potential in K562 cells pretreated with indicated concentrations of compound **1** (representative of three independent experiments). (B) The cleavage of caspase-3 and caspase-9 in K562 cells pretreated with indicated concentrations of compound **1**. Fifty μg of total proteins (per lane) was loaded to 10% gel electrophoresis followed by immunoblotting with caspase-3 and caspase-9 antibodies, respectively. (C) The ROS generation in K562 cells pretreated with serial concentrations of compound **1**.

the reduction of mitochondrial membrane potential. We measured the $\Delta\Psi$m difference of K562 cells with or without the treatment of the compound. The experiment was carried out using the fluorescent dye JC-1 (5,5′,6,6′-tetrachloro-1,1′,3,3′-tetraethylbenzimidazolylcarbocyanine iodide) that can accumulate in mitochondria with normal membrane potential where it forms aggregates and fluoresces red at 590 nm. It remains outside the mitochondria under abnormal $\Delta\Psi$m and exhibits as monomers that fluoresces green at 527 nm.[16] Compared with the control sample, K562 cells incubated with compound **1** exhibited a concentration-dependent reduction of JC-1 aggregates, indicating a drop in mitochondrial membrane potential of the cancer cells (Figure 6A).

Activation of Caspases. Caspases are a family of cysteine proteases which play essential roles in apoptosis, necrosis, and inflammation. To test whether compound **1** can activate caspases, we detected the cleavage of caspase-3 and caspase-9 by immunoblotting. As shown in Figure 6B, conspicuous cleavage of caspase-3 and caspase-9 could be detected at 25 μM compound **1**, which was consistent with the previous observation that some inhibitors of antiapoptotic proteins (e.g., **14**, obatoclax, TW-37, MNB) can induce the activation of caspases.[4,13,17,18]

Generation of Reactive Oxygen Species (ROS). To study other effects that may be induced by compound **1**, we used DCFH-DA (2′,7′-dichlorofluorescein diacetate) to quantify the amount of intracellular ROS. K562 cells were incubated with 10 μM DCFH-DA. DCFH-DA is transported across the cell membrane and deacetylated by esterases to form nonfluorescent DCFH (2′,7′-dichlorohydrofluorescein). DCFH is trapped inside the cells and oxidized by ROS to a highly fluorescent DCF (2′,7′-dichlorofluorescein).[19] The elevation of ROS level in cells thus can be quantified by the fluorescence intensity of DCF. As shown in Figure 6C, the mean fluorescence intensity per cell was increased by 2.7-fold with 25 μM compound **1** compared to that of nontreated cells, indicating that compound **1** had induced the ROS generation. In addition, the ROS generation is dependent on the compound concentration. Our result is consistent with the previous report that inhibitors of antiapoptotic proteins such as **14** can stimulate the ROS generation.[20]

Conclusion

Since the discovery of the Bcl-2 gene 20 years ago,[21] tremendous efforts had been focused on the identification of Bcl-2 family members and characterization of their functions. The determination of the 3D structures of Bcl-x_L and its complex with the Bak BH3 domain peptide contributed to the development of the inhibitors for antiapoptotic proteins of this family. Since high expression of Bcl-2 or Bcl-x_L is associated with a more aggressive malignant phenotype and/or chemoresistance in hemotologic malignancies and solid tumors,[22−25] the development of Bcl-x_L or Bcl-2 inhibitors is of particular interest in cancer chemotherapy. In the present study, we discovered a quinazoline-2(1*H*)-thione derivative as a new Bcl-x_L, Bcl-2, and Mcl-1 inhibitor by computer virtual screening. A series of quinazoline-2(1*H*)-thione derivatives were designed and synthesized based on the chemical structure of the hit compound **1**. All of the compounds were evaluated by the FP assay for their inhibitory activities against Bcl-x_L. Twenty-two compounds (**1a**−**1d**, **7**−**13**, and **12a**−**12i**) showed a Bcl-x_L inhibitory activity with IC_{50} values of 1.9−72.0 μM. The structure−activity relationship of these compounds was established, and their binding models with Bcl-x_L were built by molecular modeling simulations and confirmed by SAR and protein mutation study.

The Bcl-2-specific inhibitor like compound **17** can cause mitochondrial outer membrane permeabilization that results in the release of cytochrome *c*, activation of caspases, and morphological changes characteristically associated with apoptosis.[14] Our compound **1** can induce caspase-3/caspase-9 activation and chromatin condensation that are normally associated with apoptosis. However, the cytotoxicity assay and the change of outer mitochondrial membrane suggest that the compounds induced cell death not solely through Bcl-2 family proteins and may target additional proteins outside the Bcl-2 family. Transmission electron microscopy and flow cytometry experiments showed that compound **1** can cause mitochondrial damage and ROS generation, which may be responsible for the induction of cell death. Much more intensive work is needed to identify the target(s) responsible for the observed cytotoxicity. Now, compound **17** is a powerful tool to specifically target Bcl-2 or Bcl-x_L and thereby give important insight into the functions of these proteins.

However, as unpredictable toxicities may exist, mechanistic studies with Bcl-2 antagonists other than **17** should be carefully considered, and the interpretation of the data might be based on nonspecific effects rather than a direct interaction with Bcl-2 proteins. Considering the higher potency of **17** compared with other inhibitors, it is possible that structural optimization of compound **1** may yield more potent and selective compounds, whose activity would be more dependent on Bcl-2 family proteins.

Experimental Section

Mutagenesis and Protein Purification. The coding region for human Bcl-x_L without the C-terminal 22 residues was amplified by PCR from the Bcl-x_L plasmid on pET32b vector. The product was then digested and ligated to the *Eco*RI/*Xho*I sites of pGEX4T-1 vector. The forward primers for mutation of E96A, Y101A, and Y195A were 5′-gaggcaggcgacgcgtttgaactgcgg-3′, 5′-gagtttgaactgcgggcccggcgggcattcag-3′, and 5′-ggatactttgtggaactcgctgggaacaatgcagcagcc-3′, respectively. The backward primers were complementary to the forward primers. The mutagenesis was carried out using the QuikChange site-directed mutagenesis kit (catalog no. 200519; Stratagene Ltd., CA) according to the protocol provided by the company. All plasmids constructed in this work were confirmed by DNA sequence analysis. *E. coli* BL21(DE3) containing the expression plasmid for Bcl-x_L or its mutant proteins were grown in LB culture medium at 37 °C with vigorous shaking (230 rpm). After the cell density reached an A_{600} of 0.6−0.8, the protein expression was induced with 1 mM isopropyl β-D-1-thiogalactopyranoside (IPTG) at 37 °C for 3 h. The cells were harvested by centrifugation at 4000 rpm for 15 min. Cell pellets were resuspended with PBS and sonicated for 30 min on ice. The crude extract was centrifuged at 15000 *g* for 30 min to remove the cell debris. The supernatant was loaded onto glutathione Sepharose resin preequilibrated with PBS. The resin was washed with 25 column volumes of PBS and eluted with 5 column volumes of the elution buffer (10 mM glutathione, 50 mM Tris, pH 8.0). The eluted fractions were dialyzed in PBS and stored at −80 °C before use.

GST-tagged mouse Mcl-1 without the N-terminal 151 residues and C-terminal 23 residues was expressed and purified as that for Bcl-x_L. His-tagged human Bcl-2 without the C-terminal 22 residues was expressed and purified following the procedures described before.[26]

Mitochondrial Membrane Potential Assay. Serial concentrations of compounds were added to 1×10^6 K562 cells. After 24 h of incubation at 37 °C, the cells were collected, washed with PBS once, and resuspended with 500 μL of JC-1 (5 μg/mL JC-1 in PBS). After 15 min of incubation at 37 °C, the cells were collected, washed with PBS twice, and resuspended in 500 μL of PBS. The fluorescence of cells was measured with FACScan (Becton Dickinson FACStar Plus flow cytometer). The excitation and emission wavelengths were 488 and 530 nm, respectively. Ten-thousand cells were analyzed per sample, and all of the experiments were conducted in triplicate.

Caspases Cleavage Assay by Western Blot. Serial concentrations of compounds were added to 1×10^6 K562 cells. After 48 h of incubation at 37 °C, the cells were collected by centrifugation at 1000 *g* for 10 min at 4 °C. The cell pellets were then washed with PBS once, resuspended in lysis buffer, and centrifuged at 15000 *g* for 10 min. The concentration of total proteins in the supernatants was determined using the BCA kit (catalog no. P0012; Beyotime Institute of Biotechnology, Shanghai, China). Fifty micrograms of total proteins were loaded on each lane of 10% gel. After electrophoresis, proteins were transferred to a PVDF membrane. Nonspecific reactivity was blocked by 5% nonfat milk prepared in TBST (10 mM Tris, 150 mM NaCl, 0.05% Tween-20, pH 7.5) at room temperature for 1 h. The membrane was then incubated with monoclonal antibody of caspase-3 (catalog no. MAB707; R&D Systems, Inc., 1:1000 dilution) and caspase-9 (catalog no. MAB8301; R&D Systems, Inc., 1:1000 dilution). The excessive antibody was washed with TBST for three times. Immune complexes were detected with horseradish perioxidase conjugated goat anti-mouse IgG antibody and visualized by using the SuperSignal West Pico kit (catalog no. 34079; Pierce, IL) according to the manufacturer's instructions.

Measurement of ROS Generation. Serial concentrations of compounds were added to 1×10^6 K562 cells. After 48 h of incubation at 37 °C, the cells were collected by centrifugation at 1000 *g* for 10 min. Then the cell pellets were washed with PBS once and resuspended in 10 μM DCFH-DA prepared in RPMI 1640 culture medium without serum. After 30 min of incubation at 37 °C, the cells were collected, washed with PBS for three times, and resuspended in PBS. The fluorescence of cells was measured with FACScan (Becton Dickinson FACStar Plus flow cytometer). Upon excitation at 488 nm, the fluorescence intensities at 530 and 585 nm, which correspond to the maximum fluorescence emission wavelengths of JC-1 monomer and aggregates, respectively, were detected. Ten-thousand cells were analyzed per sample, and all of the experiments were conducted in triplicate.

Chemistry. The reagents (chemicals) were purchased from Lancaster, Acros, and Shanghai Chemical Reagent Co. and used without further purification. Analytical thin-layer chromatography (TLC) was HSGF 254 (150−200 μm thickness; Yantai Huiyou Co., China). Nuclear magnetic resonance (NMR) spectroscopy was performed on a Bruker AMX-400 and AMX-300 NMR (IS as TMS). Chemical shifts were reported in parts per million (ppm, δ) downfield from tetramethylsilane. Proton coupling patterns were described as singlet (s), doublet (d), triplet (t), quartet (q), multiplet (m), and broad (br). Low- and high-resolution mass spectra (LRMS and HRMS) were given with electric, electrospray, and matrix-assisted laser desorption ionization (EI, ESI, and MALDI) produced by a Finnigan MAT-95, LCQ-DECA spectrometer and IonSpec 4.7 T. The purity of final compounds was assessed by the analytical HPLC method and found to be ≥95%. An Agilent 1100 series HPLC with an Agilent Zorbax Exlipse SB-C_{18} (25 × 4.6 mm, 5 μm particle size) reversed-phase column was used for analytical HPLC analyses. The elution buffer was an A/B gradient, where A = H_2O and B = CH_3OH. A Shimadzu LC 20 with CHIRALPAK AD-H (25 × 4.6 mm, 5 μm particle size) column was used for chiral chromatography separation. The elution buffer was an A/B/C gradient, where A = H_2O, B = CH_3OH, and C = HOAc. Optical rotations were reported as follows: $[\alpha]_D^{22}$ (*c* g/100 mL, in solvent).

2-(2-Methoxybenzylidene)-1-tetralone (3a). Representative Procedure for 3a−3p. A mixture of 3.5 g (0.02 mol) of l-tetralone and 2.0 g (0.02 mol) of 2-methoxyaldehyde was added slowly to 15 mL of 4% ethanolic potassium hydroxide solution at room temperature. After being stirred at room temperature for 4 h, the deposited crystals were removed by filtration and washed with dilute ethanol. The filtrate was then crystallized by ethanol to give **3a** as a white solid. Yield: 95.2%. ^{1}H NMR ($CDCl_3$): δ 8.15 (d, 1H, J = 7.8 Hz), 8.02 (s, 1H), 7.51−7.47 (m, 1H), 7.39−7.24 (m, 4H), 7.00−6.94 (m, 2H), 3.88 (s, 3H), 3.08−3.04 (m, 2H), 2.97−2.93 (m, 2H).

2-Benzylidene-1-tetralone (3b). In the same manner as described in the preparation of **3a**, **3b** was prepared from l-tetralone and benzaldehyde. Yield: 94.3%. ^{1}H NMR ($CDCl_3$): δ 8.16−8.13 (m, 1H), 7.88 (s, 1H), 7.52−7.34 (m, 7H), 7.27−7.24 (m, 1H), 3.17−3.12 (m, 2H), 2.97−2.93 (m, 2H).

2-(2-Fluorobenzylidene)-1-tetralone (3c). In the same manner as described in the preparation of **3a**, **3c** was prepared from l-tetralone and 2-fluorobenzaldehyde. Yield: 96.2%. ^{1}H NMR ($CDCl_3$): δ 8.17−8.12 (m, 1H), 7.89 (s, 1H), 7.58−7.32 (m, 4H), 7.29−7.23 (m, 3H), 3.17−3.10 (m, 2H), 2.98−2.94 (m, 2H).

2-(3-Fluorobenzylidene)-1-tetralone (3d). In the same manner as described in the preparation of **3a**, **3d** was prepared from

l-tetralone and 3-fluorobenzaldehyde. Yield: 92.2%. ^{1}H NMR ($CDCl_3$): δ 8.13 (d, 1H, J = 8.1 Hz), 7.82 (s, 1H), 7.54−7.36 (m, 3H), 7.28−7.03 (m, 4H), 3.16−3.10 (m, 2H), 3.00−2.94 (m, 2H).

2-(4-Fluorobenzylidene)-1-tetralone (3e). In the same manner as described in the preparation of **3a**, **3e** was prepared from l-tetralone and 4-fluorobenzaldehyde. Yield: 92.7%. ^{1}H NMR ($CDCl_3$): δ 8.14 (d, 1H, J = 8.1 Hz), 7.84 (s, 1H), 7.54−7.25 (m, 5H), 7.21−7.09 (m, 2H), 3.14−3.09 (m, 2H), 2.99−2.92 (m, 2H).

2-(3-Nitrobenzylidene)-1-tetralone (3f). In the same manner as described in the preparation of **3a**, **3f** was prepared from l-tetralone and 3-nitrobenzaldehyde. Yield: 93.5%. ^{1}H NMR ($CDCl_3$): δ 8.29 (s, 1H), 8.24−8.20 (m, 1H), 8.15 (d, 1H, J = 8.1 Hz), 7.86 (s, 1H), 7.75−7.73 (m, 1H), 7.65−7.37 (m, 3H), 7.32−7.27 (m, 1H), 3.21−3.10 (m, 2H), 3.03−2.96 (m, 2H).

2-(Naphthalen-1-ylmethylene)-1-tetralone (3g). In the same manner as described in the preparation of **3a**, **3g** was prepared from l-tetralone and 1-naphthaldehyde. Yield: 97.7%. ^{1}H NMR ($CDCl_3$): δ 8.15−8.13 (m, 1H), 7.88 (s, 1H), 7.50−7.34 (m, 8H), 7.27−7.34 (m, 2H), 3.16−3.12 (m, 2H), 2.98−2.93 (m, 2H).

2-(Furan-2-ylmethylene)-1-tetralone (3h). In the same manner as described in the preparation of **3a**, **3h** was prepared from l-tetralone and furan-2-carbaldehyde. Yield: 98.2%. ^{1}H NMR ($CDCl_3$): δ 8.16−8.13 (m, 1H), 7.88 (s, 1H), 7.50−7.31 (m, 5H), 7.27−7.24 (m, 1H), 3.17−3.12 (m, 2H), 2.98−2.93 (m, 2H).

2-(2-Methoxybenzylidene)-6-methoxy-1-tetralone (3i). In the same manner as described in the preparation of **3a**, **3i** was prepared from 6-methoxy-l-tetralone and 2-methoxyaldehyde. Yield: 93.7%. ^{1}H NMR ($CDCl_3$): δ 8.13 (d, 1H, J = 8.7 Hz), 7.96 (s, 1H), 7.36−7.27 (m, 2H), 7.00−76.86 (m, 3H), 6.70 (d, 1H, J = 2.1 Hz), 3.82 (s, 3H), 3.69 (s, 3H), 3.87−3.82 (m, 2H), 2.93−2.89 (m, 2H).

2-(2-Methoxybenzylidene)-5-(benzyloxy)-1-tetralone (3j). In the same manner as described in the preparation of **3a**, **3j** was prepared from 5-(benzyloxy)-1-tetralone and 2-methoxyaldehyde. Yield: 87.2%. ^{1}H NMR ($CDCl_3$): δ 7.96 (s, 1H), 7.80 (d, 1H, J = 6.6 Hz), 7.43−7.24 (m, 8H), 7.08 (d, 1H, J = 7.8 Hz), 6.99−6.91 (m, 2H), 5.10 (s, 2H), 3.84 (s, 3H), 3.04−2.99 (m, 4H).

2-(2-Methoxybenzylidene)-5-(biphenyl-2-carboxylate)-1-tetralone (3k). In the same manner as described in the preparation of **3a**, **3k** was prepared from 5-(biphenyl-2-carboxylate)-1-tetralone and 2-methoxyaldehyde. Yield: 80.2%. ^{1}H NMR ($CDCl_3$): δ 8.04 (d, 2H, J = 7.8 Hz), 7.92 (d, 2H, J = 7.5 Hz), 7.67−7.62 (m, 2H), 7.55−7.38 (m, 5H), 7.30−7.24 (m, 4H), 7.03 (d, 2H, J = 7.8 Hz), 3.83(s, 3H), 2.63−2.59 (m, 2H), 2.07−2.01 (m, 2H).

(2,6-Bis(3-fluorobenzylidene)cyclohexanone (3l). In the same manner as described in the preparation of **3a**, **3l** was prepared from cyclohexanone (0.01 mol) and 3-fluorobenzaldehyde (0.02 mol). Yield: 90.5%. ^{1}H NMR ($CDCl_3$): δ 7.74 (d, 1H, J = 7.8 Hz), 7.63−7.56 (m, 2H), 7.40−7.20 (m, 4H), 7.09 (d, 1H, J = 8.1 Hz), 2.95−2.90 (m, 4H), 1.86−1.78 (m, 2H).

3-(2-Methoxyphenyl)-1-phenylprop-2-en-1-one (3m). In the same manner as described in the preparation of **3a**, **3m** was prepared from acetophenone and 2-methoxybenzaldehyde. Yield: 99.1%. ^{1}H NMR ($CDCl_3$): δ 8.33 (m, 1H), 7.90−7.79 (m, 3H), 7.65−7.35 (m, 3H), 7.21−6.98 (m, 4H), 3.74 (m, 3H).

2-(3-Methoxybenzylidene)-1-tetralone (3n). In the same manner as described in the preparation of **3a**, **3n** was prepared from 1-tetralone and 3-methoxybenzaldehyde. Yield: 96.4%. ^{1}H NMR ($CDCl_3$): δ 8.17 (d, 1H, J = 7.8 Hz), 7.82 (s, 1H), 7.48−7.03 (m, 4H), 6.91−6.87 (m, 2H), 6.73−6.971 (m, 2H), 3.86 (s, 3H), 3.16−3.08 (m, 2H), 2.97−2.912 (m, 2H).

2-(4-Methoxybenzylidene)-1-tetralone (3o). In the same manner as described in the preparation of **3a**, **3o** was prepared from 1-tetralone and 4-methoxybenzaldehyde. Yield: 96.8%. ^{1}H NMR ($CDCl_3$): δ 8.13 (d, 1H, J = 7.8 Hz), 7.86 (s, 1H), 7.51−7.34 (m, 4H), 7.25 (d, 1H, J = 7.8 Hz), 6.97−6.94 (d, 1H, J = 8.1 Hz), 3.86 (s, 3H), 3.18−3.13 (m, 2H), 2.98−2.93 (m, 2H).

(3-Fluorobenzylidene)-6-methoxy-1-tetralone (3p). In the same manner as described in the preparation of **3a**, **3p** was prepared from 6-methoxy-1-tetralone and 4-fluorobenzaldehyde. Yield: 97.8%. ^{1}H NMR ($CDCl_3$): δ 8.14 (d, 1H, J = 7.8 Hz), 7.78 (s, 1H), 7.42−7.02 (m, 5H), 6.91−6.87 (m, 2H), 6.73−6.971 (m, 1H), 3.88 (s, 3H), 3.12−3.07 (m, 2H), 2.96−2.91 (m, 2H).

4-(2-Methoxyphenyl)-3,4,5,6-tetrahydrobenzo[*h*]quinazoline-2(1*H*)-thione (4a) and 7-(2-Methoxyphenyl)-7,10-dihydro-5*H*-benzo[*h*]thiazolo[2,3-*b*]quinazolin-9(6*H*)-one (5a). Representative Procedure for 4a−4p and 5a−5p. A mixture of 2-(2-methoxybenzylidene)-tetralone (**3a**, 0.02 mol) and thiourea (0.02 mol) in ethanolic KOH (2.0 g of KOH in 75 mL of ethanol) was heated under reflux for 5 h. The volume of the reaction mixture was reduced to half and kept overnight. The solid thus separated as shining needles, was filtered, and washed with aqueous ethanol to give **4a** as a yellow solid. A mixture of **4a** (0.01 mol), chloroacetic acid (0.01 mol), anhydrous sodium acetate (0.01 mol), acetic acid (10 mL), and acetic anhydride (2 mL) was heated under reflux for 2 h. The reaction mixture was cooled and poured into ice−water while stirring. The solid thus separated was filtered, washed with water, and finally crystallized from acetic acid to give **5a** as a red solid. Yield: 71.2%. ^{1}H NMR ($CDCl_3$): δ 7.94 (d, 1H, J = 7.5 Hz), 7.30−7.24 (m, 3H), 7.20−7.15 (m, 1H), 7.09−7.06 (m, 1H), 6.95−6.89 (m, 2H), 5.97 (s, 1H), 3.87 (s, 3H), 3.86−3.68 (dd, 2H), 2.84−2.74 (m, 1H), 2.84−2.74 (m, 1H), 2.69−2.56 (m, 1H), 2.10−1.98 (m, 1H).

7-Phenyl-7,10-dihydro-5*H*-benzo[*h*]thiazolo[2,3-*b*]quinazolin-9(6*H*)-one (5b). In the same manner as described in the preparation of **5a**, **5b** was prepared from 2-benzylidene-1-tetralone (**3b**). Yield: 72.3%. ^{1}H NMR ($CDCl_3$): δ 7.97 (d, 1H, J = 7.5 Hz), 7.44−7.09 (m, 8H), 5.58 (s, 1H), 3.88−3.70 (dd, 2H), 2.82−2.68 (m, 2H), 2.24−2.06 (m, 2H).

7-(2-Fluorophenyl)-7,10-dihydro-5*H*-benzo[*h*]thiazolo[2,3-*b*]-quinazolin-9(6*H*)-one (5c). In the same manner as described in the preparation of **5a**, **5c** was prepared from 2-(2-fluorobenzylidene)-1-tetralone (**3c**). Yield: 74.4%. ^{1}H NMR ($CDCl_3$): δ 7.96 (d, 1H, J = 7.8 Hz), 7.41−7.25 (m, 3H), 7.23−7.03 (m, 4H), 5.92 (s, 1H), 3.88−3.72 (dd, 2H), 2.88−2.66 (m, 2H), 2.36−2.04 (m, 2H).

7-(3-Fluorophenyl)-7,10-dihydro-5*H*-benzo[*h*]thiazolo[2,3-*b*]-quinazolin-9(6*H*)-one (5d). In the same manner as described in the preparation of **5a**, **5d** was prepared from 2-(3-fluorobenzylidene)-1-tetralone (**3d**). Yield: 70.9%. ^{1}H NMR ($CDCl_3$): δ 7.96 (d, 1H, J = 7.5 Hz), 7.36−6.99 (m, 7H), 5.57 (s, 1H), 3.88−3.72 (dd, 2H), 2.86−2.69 (m, 2H), 2.26−2.04 (m, 2H).

7-(4-Fluorophenyl)-7,10-dihydro-5*H*-benzo[*h*]thiazolo[2,3-*b*]-quinazolin-9(6*H*)-one (5e). In the same manner as described in the preparation of **5a**, **5e** was prepared from 2-(4-fluorobenzylidene)-1-tetralone (**3e**). Yield: 70.8%. ^{1}H NMR ($CDCl_3$): δ 7.96 (d, 1H, J = 7.8 Hz), 7.35−7.27 (m, 2H), 7.23−7.10 (m, 2H), 7.15−6.99 (m, 3H), 5.57 (s, 1H), 3.88−3.72 (dd, 2H), 2.86−2.69 (m, 2H), 2.26−2.04 (m, 2H).

7-(3-Nitrophenyl)-7,10-dihydro-5*H*-benzo[*h*]thiazolo[2,3-*b*]-quinazolin-9(6*H*)-one (5f). In the same manner as described in the preparation of **5a**, **5f** was prepared from 2-(3-nitrobenzylidene)-1-tetralone (**3f**). Yield: 68.8%. ^{1}H NMR ($CDCl_3$): δ 8.30−8.28 (m, 1H), 8.22−8.18 (m, 1H), 7.98−7.96 (m, 1H), 7.79−7.15 (m, 1H), 7.58−7.52 (m, 1H), 7.34−7.21 (m, 2H), 7.13−7.10 (m, 1H), 5.57 (s, 1H), 3.88−3.72 (dd, 2H), 2.86−2.69 (m, 2H), 2.26−2.04 (m, 2H).

7-(Naphthalen-1-yl)-7,10-dihydro-5*H*-benzo[*h*]thiazolo[2,3-*b*]-quinazolin-9(6*H*)-one (5g). In the same manner as described in the preparation of **5a**, **5g** was prepared from 2-(naphthalen-1-ylmethylene)-1-tetralone (**3g**). Yield: 72.3%. ^{1}H NMR ($CDCl_3$): δ 8.00−7.81 (m, 5H), 7.53−7.48 (m, 3H), 7.34−7.09 (m, 3H), 5.75 (s, 1H), 3.88−3.68 (dd, 2H), 2.80−2.68 (m, 2H), 2.28−2.04 (m, 2H).

7-(Furan-2-yl)-7,10-dihydro-5*H*-benzo[*h*]thiazolo[2,3-*b*]-quinazolin-9(6*H*)-one (5h). In the same manner as described in the preparation of **5a**, **5h** was prepared from 2-(furan-2-ylmethylene)-1-tetralone (**3h**). Yield: 62.3%. ^{1}H NMR ($CDCl_3$): δ 7.94−7.92

(m, 1H), 7.35−7.11 (m, 4H), 6.44−6.33 (m, 2H), 5.53 (s, 1H), 3.88−3.83 (dd, 2H), 2.86−2.78 (m, 2H), 2.25−2.11 (m, 2H).

3-Methoxy-7-(2-methoxyphenyl)-7,10-dihydro-5*H*-benzo[*h*]-thiazolo[2,3-*b*]quinazolin-9(6*H*)-one (5i). In the same manner as described in the preparation of **5a**, **5i** was prepared from 2-(2-methoxybenzylidene)-5-(benzyloxy)-1-tetralone (**3i**). Yield: 62.3%. ^{1}H NMR ($CDCl_3$): δ 7.63−7.60 (m, 1H), 7.32−7.21 (m, 2H), 7.01−6.97 (m, 2H), 6.78−6.75 (m, 2H), 5.32 (s, 1H), 3.81 (s, 3H), 3.75 (s, 3H), 3.74−3.69 (dd, 2H), 2.72−2.51 (m, 2H), 2.20−2.10 (m, 1H), 1.91−1.80 (m, 1H).

4-(Benzyloxy)-7-(2-methoxyphenyl)-7,10-dihydro-5*H*-benzo[*h*]-thiazolo[2,3-*b*]quinazolin-9(6*H*)-one (5j). In the same manner as described in the preparation of **5a**, **5j** was prepared from 2-(2-methoxybenzylidene)-5-(benzyloxy)-1-tetralone (**3j**). Yield: 65.3%. ^{1}H NMR ($CDCl_3$): δ 7.65−7.63 (m, 1H), 7.54−7.14 (m, 8H), 6.95−6.68 (m, 3H), 5.97 (s, 1H), 5.13 (s, 2H), 3.85 (s, 3H), 3.84−3.74 (dd, 2H), 2.82−2.75 (m, 2H), 2.36−1.98 (m, 2H).

7-(2-Methoxyphenyl)-9-oxo-6,7,9,10-tetrahydro-5*H*-benzo[*h*]-thiazolo[2,3-*b*]quinazolin-4-ylbiphenyl-2-carboxylate (5k). In the same manner as described in the preparation of **5a**, **5k** was prepared from 2-(2-methoxybenzylidene)-5-(biphenyl-2-carboxylate)-1-tetralone (**3k**). Yield: 62.3%. ^{1}H NMR ($CDCl_3$): δ 7.96 (d, 1H, J = 7.5 Hz), 7.82 (d, 1H, J = 7.5 Hz), 7.61−7.56 (m, 1H), 7.49−7.33 (m, 6H), 7.29−7.17 (m, 4H), 6.95−6.87 (m, 2H), 6.70 (d, 1H, J = 8.1 Hz), 5.54 (s, 1H), 3.99 (s, 3H), 3.97−3.68 (dd, 2H), 2.46−2.34 (m, 2H), 2.12−2.09 (m, 1H), 1.98−1.92 (m, 1H).

(*E*)-9-(3-Fluorobenzylidene)-5-(3-fluorophenyl)-6,7,8,9-tetrahydro-2*H*-thiazolo[2,3-*b*]quinazolin-3(5*H*)-one (5l). In the same manner as described in the preparation of **5a**, **5l** was prepared from 2,6-bis(3-fluorobenzylidene)cyclohexanone (**3l**). Yield: 67.3%. ^{1}H NMR ($CDCl_3$): δ 7.71 (d, 1H, J = 7.8 Hz), 7.63−7.56 (m, 2H), 7.39−7.11 (m, 4H), 7.10 (d, 1H, J = 8.1 Hz), 5.17 (s, 1H), 3.04−3.00 (m, 2H), 2.68−2.64 (m, 2H), 2.20−2.13 (m, 2H).

5-(2-Methoxyphenyl)-7-phenyl-2*H*-thiazolo[3,2-*a*]pyrimidin-3(5*H*)-one (5m). In the same manner as described in the preparation of **5a**, **5m** was prepared from 3-(2-methoxyphenyl)-1-phenyl-prop-2-en-1-one (**3m**). Yield: 62.8%. ^{1}H NMR ($CDCl_3$): δ 7.92−7.64 (m, 3H), 7.57−7.35 (m, 2H), 7.57−7.35 (m, 2H), 7.06 −6.96 (m, 2H), 6.01 (d, 1H, J = 4.2 Hz), 5.91 (d, 1H, J = 4.2 Hz), 3.74 (m, 3H), 3.87−3.73 (dd, 2H).

7-(3-Methoxyphenyl)-7,10-dihydro-5*H*-benzo[*h*]thiazolo[2,3-*b*]-quinazolin-9(6*H*)-one (5n). In the same manner as described in the preparation of **5a**, **5n** was prepared from 2-(3-methoxybenzylidene)-1-tetralone (**3n**). Yield: 73.3%. ^{1}H NMR ($CDCl_3$): δ 7.97 (d, 1H, J = 8.4 Hz), 7.36−7.10 (m, 4H), 6.83−6.79 (m, 2H), 6.83−6.79 (m, 2H), 5.56 (s, 1H), 3.89−3.72 (dd, 2H), 3.83 (s, 3H), 2.780−2.67 (m, 2H), 2.21−2.03 (m, 2H).

7-(4-Methoxyphenyl)-7,10-dihydro-5*H*-benzo[*h*]thiazolo[2,3-*b*]-quinazolin-9(6*H*)-one (5o). In the same manner as described in the preparation of **5a**, **5o** was prepared from 2-(4-methoxybenzylidene)-1-tetralone (**3o**). Yield: 74.8%. ^{1}H NMR ($CDCl_3$): δ 7.95 (d, 1H, J = 7.5 Hz), 7.36−7.29 (m, 3H), 7.23−7.17 (m, 1H), 7.11−7.09 (m, 1H), 6.89−6.84 (m, 2H), 5.54 (s, 1H), 3.86−3.68 (dd, 2H), 3.80 (s, 3H), 2.86−2.65 (m, 2H), 2.25−2.01 (m, 2H).

3-Methoxy-7-(3-fluorophenyl)-7,10-dihydro-5*H*-benzo[*h*]-thiazolo[2,3-*b*]quinazolin-9(6*H*)-one (5p). In the same manner as described in the preparation of **5a**, **5p** was prepared from (3-fluorobenzylidene)-6-methoxy-1-tetralone (**3p**). Yield: 75.5%; ^{1}H NMR ($CDCl_3$): δ 7.86 (d, 1H, J = 8.4 Hz), 7.33−7.00 (m, 5H), 6.83−6.79 (m, 1H), 6.67 (d, 1H, J = 2.4 Hz), 5.55 (s, 1H), 3.88−3.71 (dd, 2H), 3.82 (s, 3H), 2.79−2.68 (m, 2H), 2.22−2.04 (m, 2H).

(*Z*)-2-(3-((7-(2-Methoxyphenyl)-9-oxo-5H-benzo[*h*]thiazolo[2,3-*b*]-quinazolin-10(6*H*,7*H*,9*H*)-ylidene)methyl)phenoxy)acetic Acid (1). Representative Procedure for 1, 1a−1i, 6−13, and 12a−12k. The mixture of thiones **5a** (1 mmol), 2-(3-formylphenoxy)acetic acid (1 mmol), and piperidine was dissolved in EtOH. The mixture was reflux for 3 h. The precipitate was collected by filtration, washed with EtOH, and purified by chromatography with CH_2Cl_2/CH_3OH (20:1 v/v) to afford the target compound **1** as a yellow solid. Yield: 70.2%. HPLC: 98.35%, t_R = 1.496 min. ^{1}H NMR (300 MHz, DMSO-d_6): δ 7.78 (d, J = 7.8 Hz, 1H), 7.54 (s, 1H), 7.42−7.36 (m, 1H), 7.29−6.90 (m, 10H), 6.01 (s, 1H), 4.51 (s, 2H), 3.79 (s, 3H), 2.77−2.69 (m, 1H), 2.60−2.52 (m, 1H), 2.32−2.22 (m, 1H), 1.93−1.83 (m, 1H). ESI-MS m/z 523 [M − H]$^-$. HRMS (EI) m/z calcd for $C_{30}H_{24}N_2O_5S$ (M^+) 524.1406, found 524.1411. Enantiomeric analysis: determined by HPLC (Chiralpak AD-H, hexane/2-propanol/HOAc = 65/35/0.1 (v/v/v), flow rate 0.5 mL/min), isomer **1-1** (*S*), t_R = 9.105 min, $[\alpha]_D^{22}$ = −40 (*c* 0.14 g/1000 mL, in CH_2Cl_2); isomer **1-2** (*R*), t_R = 13.123 min, $[\alpha]_D^{22}$ = −11 (*c* 0.10 g/100 mL, in CH_2Cl_2).

(*Z*)-Ethyl-2-(3-((7-(2-methoxyphenyl)-9-oxo-5*H*-benzo[*h*]-thiazolo[2,3-*b*]quinazolin-10(6*H*,7*H*,9*H*)-ylidene)methyl)phenoxy)-acetate (6). In the same manner as described in the preparation of **1**, compound **6** was prepared from **5a** and ethyl 2-(3-formylphenoxy)acetate. Yield: 61.2%. HPLC: 95.22%, t_R = 10.653 min. ^{1}H NMR (300 MHz, $CDCl_3$): δ 7.95 (d, 1H, J = 7.8 Hz), 7.93 (s, 1H), 7.41−7.08 (m, 7H), 7.01−6.89 (m, 4H), 6.10 (s, 1H), 4.67 (s, 2H), 4.35−4.28 (q, 2H), 3.86 (s, 3H), 2.82−2.77 (m, 1H), 2.72−2.64 (m, 1H), 2.32−2.25 (m, 1H), 2.15−2.06 (m, 1H), 1.34 (t, 3H). EI-MS m/z 552 (M). HRMS (EI) m/z calcd for $C_{32}H_{28}N_2O_5S$ (M^+) 552.1719, found 552.1723.

(*Z*)-2-(2-((7-(2-Methoxyphenyl)-9-oxo-5*H*-benzo[*h*]thiazolo-[2,3-*b*]quinazolin-10(6*H*,7*H*,9*H*)-ylidene)methyl)phenoxy)acetic Acid (7). In the same manner as described in the preparation of **1**, compound **7** was prepared from **5a** and 2-(2-formylphenoxy)acetic acid. Yield: 54.8%. HPLC: 96.21%, t_R = 1.876 min. ^{1}H NMR (300 MHz, DMSO-d_6): δ 7.81 (d, 1H, J = 7.5 Hz), 7.60−7.55 (t, 3H), 7.31−6.93 (m, 9H), 6.06 (s, 1H), 4.80 (s, 2H), 3.76 (s, 3H), 2.79−2.72 (m, 1H), 2.63−2.52 (m, 1H), 2.36−2.23 (m, 1H), 2.19−1.85 (m, 1H). ESI-MS m/z 523 [M − H]$^-$. HRMS (EI) m/z calcd for $C_{30}H_{24}N_2O_5S$ (M^+) 524.1406, found 524.1413.

(*Z*)-2-(4-((7-(2-Methoxyphenyl)-9-oxo-5*H*-benzo[*h*]thiazolo[2,3-*b*]-quinazolin-10(6*H*,7*H*,9*H*)-ylidene)methyl)phenoxy)acetic Acid (8). In the same manner as described in the preparation of **1**, compound **8** was prepared from **5a** and 2-(4-formylphenoxy)acetic acid. Yield: 73.3%. HPLC: 96.62%, t_R = 1.747 min. ^{1}H NMR (300 MHz, DMSO-d_6): δ 7.92 (s, 1H), 7.78 (d, 1H, J = 7.5 Hz), 7.44−7.41 (m, 1H), 7.38−6.85 (m, 10H), 56.06 (s, 1H), 4.26 (s, 2H), 3.76 (s, 3H), 2.78−2.73 (m, 1H), 2.71−2.54 (m, 1H), 2.35−2.18 (m, 1H), 1.96−1.76 (m, 1H). ESI-MS m/z 523 [M − H]$^-$. HRMS (EI) m/z calcd for $C_{30}H_{24}N_2O_5S$ (M^+) 524.1406, found 524.1411.

(*Z*)-3-(4-((*E*)-(7-(2-Methoxyphenyl)-9-oxo-5*H*-benzo[*h*]thiazolo-[2,3-*b*]quinazolin-10(6*H*,7*H*,9H)-ylidene)methyl)phenyl)acrylic Acid (9). In the same manner as described in the preparation of **1**, compound **9** was prepared from **5a** and (*E*)-3-(4-formylphenyl)acrylic acid. Yield: 89.8%. HPLC: 100.00%, t_R = 4.246 min. ^{1}H NMR (300 MHz, DMSO-d_6): δ 7.91−7.67 (m, 3H), 7.62−7.57 (m, 4H), 7.29−6.90 (m, 7H), 6.72−6.59 (m, 1H), 6.04 (s, 1H), 6.03 (s, 1H), 3.70 (s, 3H), 2.78−2.69 (m, 1H), 2.60−2.47 (m, 1H), 2.33−2.22 (m, 1H), 1.97−1.82 (m, 1H). ESI-MS m/z 519 [M − H]$^-$. HRMS (EI) m/z calcd for $C_{31}H_{24}N_2O_4S$ [M^+] 520.1457, found 520.1449.

(*Z*)-4-((7-(2-Methoxyphenyl)-9-oxo-5*H*-benzo[*h*]thiazolo[2,3-*b*]-quinazolin-10(6*H*,7*H*,9*H*)-ylidene)methyl)benzoic Acid (10). In the same manner as described in the preparation of **1**, **10** was prepared from **5a** and 4-formylbenzoic acid. Yield: 92.5%. HPLC: 100.00%, t_R = 3.076 min. ^{1}H NMR (300 MHz, DMSO-d_6): δ 8.05−8.03 (d, 2H, J = 8.4 Hz), 7.79−7.65 (m, 4H), 7.30−6.90 (m, 7H), 6.04 (s, 1H), 3.72 (s, 3H), 2.78−2.69 (m, 1H), 2.61−2.47 (m, 1H), 2.34−2.23 (m, 1H), 1.97−1.823 (m, 1H). ESI-MS m/z 493 [M − H]$^-$. HRMS (EI) m/z calcd for $C_{29}H_{22}N_2O_4S$ [M^+] 494.1300, found 494.1308.

(*Z*)-3′-((7-(2-Methoxyphenyl)-9-oxo-5*H*-benzo[*h*]thiazolo[2,3-*b*]-quinazolin-10(6*H*,7*H*,9*H*)-ylidene)methyl)biphenyl-3-carboxylic Acid (11). In the same manner as described in the preparation of **1**, **13** was prepared from **5a** and 3′-formylbiphenyl-3-carboxylic acid. Yield: 90.1%. HPLC: 100.00%, t_R = 5.371 min. ^{1}H NMR (300 MHz, DMSO-d_6): δ 8.26 (s, 1H), 7.97−7.53 (m, 10H),

7.49−6.93 (m, 6H), 6.07 (s, 1H), 3.76 (s, 3H), 2.89−2.51 (m, 2H), 2.36−2.25 (m, 1H), 2.08−1.96 (m, 1H). ESI-MS *m*/*z* 569 [M − H]$^-$. HRMS (EI) *m*/*z* calcd for $C_{35}H_{26}N_2O_4S$ [M$^+$] 570.1613, found 570.1624.

(*Z*)-3-(5-((7-(2-Methoxyphenyl)-9-oxo-5*H*-benzo[*h*]thiazolo[2,3-*b*]-quinazolin-10(6*H*,7*H*,9*H*)-ylidene)methyl)furan-2-yl)benzoic Acid (12). In the same manner as described in the preparation of **1**, **12** was prepared from **5a** and 3-(5-formylfuran-2-yl)benzoic acid. Yield: 88.2%. HPLC: 100.00%, t_R = 4.874 min. ^{1}H NMR (300 MHz, DMSO-d_6): δ 8.34 (s, 1H), 7.93−7.82 (m, 3H), 7.54−7.48 (m, 2H), 7.30−7.01 (m, 7H), 7.04−7.10 (m, 2H), 6.04 (s, 1H), 3.72 (s, 3H), 3.02−2.98 (m, 1H), 2.80−2.71 (m, 1H), 2.35−2.24 (m, 1H), 1.94−1.87 (m, 1H). ESI-MS *m*/*z* 559 [M − H]$^-$. HRMS (EI) *m*/*z* calcd for $C_{33}H_{24}N_2O_5S$ [M$^+$] 560.1406, found 560.1413.

(*Z*)-3-((2-Methoxy-4-((7-(4-methoxyphenyl)-9-oxo-5*H*-benzo[*h*]-thiazolo[2,3-b]quinazolin-10(6*H*,7*H*,9*H*)-ylidene)methyl)phenoxy)-methyl)benzoic Acid (13). In the same manner as described in the preparation of **1**, **13** was prepared from **5p** and 3-((4-formyl-2-methoxy-phenoxy)methyl)benzoic acid. Yield: 87.2%. HPLC: 100.00%, t_R = 8.740 min. ^{1}H NMR (300 MHz, DMSO-d_6): δ 8.03 (s, 1H), 7.92−7.51 (m, 5H), 7.33−7.12 (m, 8H), 6.93−6.88 (m, 2H), 5.79 (s, 1H), 5.26 (s, 2H), 3.84 (s, 3H), 3.71 (s, 3H), 2.83−2.58 (m, 2H), 2.36−2.24 (m, 1H), 1.99−1.88 (m, 1H). ESI-MS *m*/*z* 629 [M − H]$^-$. HRMS (EI) *m*/*z* calcd for $C_{37}H_{30}N_2O_6S$ [M$^+$] 630.1825, found 630.1834.

(*Z*)-2-(3-((9-Oxo-7-phenyl)-5*H*-benzo[*h*]thiazolo[2,3-*b*]quinazolin-10(6*H*,7*H*,9*H*)-ylidene)methyl)phenoxy)acetic Acid (1a). In the same manner as described in the preparation of **1**, **1a** was prepared from **5b** and 2-(3-formylphenoxy)acetic acid. Yield: 80.2.%. HPLC: 100.00%, t_R = 2.376 min. ^{1}H NMR (DMSO-d_6): δ 7.66 (s, 1H), 7.47−7.36 (m, 4H), 7.23−6.97 (m, 9H), 5.78 (s, 1H), 4.75 (s, 2H), 2.71−2.66 (m, 1H), 2.54−2.49 (m, 1H), 2.26−2.20 (m, 1H), 1.87−1.81 (m, 1H). ESI-MS *m*/*z* 493 [M − H]$^-$. HRMS (EI) *m*/*z* calcd for $C_{29}H_{22}N_2O_4S$ [M$^+$] 494.1300, found 494.1310.

(*Z*)-2-(3-((7-(3-Fluorophenyl)-9-oxo-5*H*-benzo[h]thiazolo[2,3-*b*]-quinazolin-10(6*H*,7*H*,9*H*)-ylidene)methyl)phenoxy)acetic Acid (1b). In the same manner as described in the preparation of **1**, **1b** was prepared from **5d** and 2-(3-formylphenoxy)acetic acid. Yield: 70.8%. HPLC: 100.00%, t_R = 1.745 min. ^{1}H NMR (DMSO-d_6): δ 7.80 (m, 1H), 7.61 (s, 1H), 7.39−6.97 (m, 11H), 5.85 (s, 1H), 4.54 (s, 2H), 2.64−2.48 (m, 2H), 2.34−2.29 (m, 1H), 1.96−1.87 (m, 1H). ESI-MS *m*/*z* 511 [M − H]$^-$. HRMS (EI) *m*/*z* calcd for $C_{29}H_{21}FN_2O_4S$ [M$^+$] 512.1206, found 512.1216.

(*Z*)-2-(3-((7-(Naphthalen-1-yl)-9-oxo-5*H*-benzo[*h*]thiazolo[2,3-*b*]-quinazolin-10(6*H*,7*H*,9*H*)-ylidene)methyl)phenoxy)acetic Acid (1c). In the same manner as described in the preparation of **1**, **1c** was prepared from **5g** and 2-(3-formylphenoxy)acetic acid. Yield: 69.8%. HPLC: 95.00%, t_R = 2.478 min. ^{1}H NMR (DMSO-d_6): δ 7.98−7.84 (m, 5H), 7.62 (s, 1H), 7.55−7.41 (m, 4H), 7.30−7.01 (m, 6H), 6.02 (s, 1H), 4.78 (s, 2H), 2.83−2.72 (m, 1H), 2.65−2.55 (m, 1H), 2.47−2.32 (m, 1H), 1.99−1.87 (m, 1H). ESI-MS *m*/*z* 543 [M − H]$^-$. HRMS (EI) *m*/*z* calcd for $C_{33}H_{24}N_2O_6S$ [M$^+$] 544.1457, found 544.1463.

(*Z*)-2-(3-((7-(Furan-2-yl)-9-oxo-5*H*-benzo[*h*]thiazolo[2,3-*b*]quinazolin-10(6*H*,7*H*,9*H*)-ylidene)methyl)phenoxy)acetic Acid (1d). In the same manner as described in the preparation of **1**, **1d** was prepared from **5h** and 2-(3-formylphenoxy)acetic acid. Yield: 73.8%. HPLC: 100.00%, t_R = 2.770 min. ^{1}H NMR (DMSO-d_6): δ 7.81 (d, 1H, *J* = 7.2 Hz), 7.63 (s, 1H), 7.47−7.36 (m, 3H), 7.30−6.99 (d, 7H), 6.07 (s, 1H), 4.50 (s, 2H), 2.86−2.75 (m, 1H), 2.67−2.57 (m, 1H), 2.37−2.23 (m, 1H), 1.97−1.88 (m, 1H). ESI-MS *m*/*z* 483 [M − H]$^-$. HRMS (EI) *m*/*z* calcd for $C_{27}H_{20}N_2O_5S$ [M$^+$] 484.1093, found 484.1101.

(*Z*)-2-(3-((3-Methoxy-7-(2-methoxyphenyl)-9-oxo-5*H*-benzo[*h*]-thiazolo[2,3-*b*]quinazolin-10(6*H*,7*H*,9*H*)-ylidene)methyl)phenoxy)-acetic Acid (1e). In the same manner as described in the preparation of **1**, **1e** was prepared from **5i** and 2-(3-formylphenoxy)acetic acid. Yield: 75.0%.; HPLC: 100.00%, t_R = 8.209 min. ^{1}H NMR (DMSO-d_6): δ 7.70 (d, 1H, *J* = 8.7 Hz), 7.59 (s, 1H), 7.48−7.42 (m, 1H), 7.30−7.28 (m, 3H), 7.25−6.91 (m, 4H), 6.81−6.78 (m, 1H), 6.71 (d, 1H, *J* = 8.7 Hz), 6.02 (s, 1H), 4.86 (s, 2H), 3.75 (s, 3H), 3.70 (s, 3H), 2.73−2.70 (m, 1H), 2.59−2.54 (m, 1H), 2.29−2.23 (m, 1H), 1.93−1.85 (m, 1H). ESI-MS *m*/*z* 553 [M − H]$^-$. HRMS (ESI) *m*/*z* calcd for $C_{31}H_{26}N_2O_6S$ [M$^+$] 554.1512, found 554.1518.

(*Z*)-2-(3-((4-(Benzyloxy)-7-(2-methoxyphenyl)-9-oxo-5*H*-benzo[h]-thiazolo[2,3-*b*]quinazolin-10(6*H*,7*H*,9*H*)-ylidene)methyl)phenoxy)-acetic Acid (1f). In the same manner as described in the preparation of **1**, **1f** was prepared from **5j** and 2-(3-formylphenoxy)acetic acid. Yield: 62.3%. HPLC: 100.00%, t_R = 2.385 min. ^{1}H NMR (300 MHz, DMSO-d_6): δ 7.59 (s, 1H), 7.49−7.35 (m, 7H), 7.29−7.27 (m, 2H), 7.24−7.21 (m, 2H,), 7.19−7.17 (m, 1H), 7.14−6.93 (m, 4H), 6.05 (s, 1H), 5.11 (s, 2H), 4.66 (s, 2H), 3.76 (s, 3H), 2.69−2.51 (m, 2H), 2.33−2.27 (m, 1H), 1.92−1.86 (m, 1H). ESI-MS *m*/*z* 629 [M − H]$^-$. HRMS (EI) *m*/*z* calcd for $C_{37}H_{30}N_2O_6S$ [M$^+$] 630.1825, found 630.1831.

(*Z*)-2-(3-((4-(Biphenylcarbonyloxy)-7-(2-methoxyphenyl)-9-oxo-5*H*-benzo[h]thiazolo[2,3-*b*]quinazolin-10(6*H*,7*H*,9*H*)-ylidene)methyl)-phenoxy)acetic Acid (1g). In the same manner as described in the preparation of **1**, **1g** was prepared from **5k** and 2-(3-formylphenoxy)acetic acid. Yield: 64.1%. HPLC: 100.00%, t_R = 4.990 min. ^{1}H NMR (300 MHz, DMSO-d_6): δ 7.96 (d, 1H, *J* = 6.6 Hz), 7.72−7.67 (m, 2H), 7.60−7.53 (m, 2H), 7.49−7.04 (m, 11H), 7.11 (s, 1H), 6.97−6.94 (d, 1H, *J* = 4.5 Hz), 6.92−6.82 (m, 1H), 6.80 (d, 1H, *J* = 6.6 Hz), 6.01 (s, 1H), 4.75 (s, 2H), 3.74 (s, 3H), 2.50−2.19 (m, 3H), 1.83−1.77 (m, 1H). ESI-MS *m*/*z* 719 [M − H]$^-$. HRMS (EI) *m*/*z* calcd for $C_{43}H_{32}N_2O_7S$ [M$^+$] 720.1930, found 720.1938.

2-(3-((*Z*)-((*E*)-9-(3-Fluorobenzylidene)-5-(3-fluorophenyl)-3-oxo-3,5,6,7,8,9-hexahydro-2*H*-thiazolo[2,3-*b*]quinazolin-2-ylidene)methyl)-phenoxy)acetic Acid (1h). In the same manner as described in the preparation of **1**, **1h** was prepared from **5l** and 2-(3-formylphenoxy)acetic acid. Yield: 66.9%. HPLC: 100.00%, t_R = 2.236 min. ^{1}H NMR (300 MHz, DMSO-d_6): δ 7.81 (d, 1H, *J* = 7.8 Hz), 7.65 (s, 1H), 7.48−7.42 (m, 1H), 7.40−7.29 (m, 5H), 7.28−7.05 (m, 4H), 7.04−7.02 (m, 4H), 5.86 (s, 1H), 4.75 (s, 2H), 2.76−2.61 (m, 2H), 2.39−2.31 (m, 1H), 1.92−1.90 (m, 1H). ESI-MS *m*/*z* 569 [M − H]$^-$. HRMS (EI) *m*/*z* calcd for $C_{32}H_{24}F_2N_2O_4S$ [M$^+$] 570.1425, found 570.1433.

(*Z*)-2-(3-((5-(2-Methoxyphenyl)-3-oxo-7-phenyl-3,5-dihydro-2*H*-thiazolo[3,2-*a*]pyrimidin-2-ylidene)methyl)phenoxy)acetic Acid (1i). In the same manner as described in the preparation of **1**, **1i** was prepared from **5m** and 2-(3-formylphenoxy)acetic acid. Yield: 63.2%. HPLC: 100.00%, t_R = 1.757 min. ^{1}H NMR (300 MHz, DMSO-d_6): δ 7.77 (d, 1H, *J* = 7.5 Hz), 7.64 (s, 1H), 7.43−7.30 (m, 5H), 7.18−6.96 (m, 7H), 6.16 (d, 1H, *J* = 4.5 Hz), 6.04 (d, 1H, *J* = 4.2 Hz), 4.44 (s, 2H), 3.83 (s, 3H). ESI-MS *m*/*z* 497 [M − H]$^-$. HRMS (EI) *m*/*z* calcd for $C_{28}H_{22}N_2O_5S$ [M$^+$] 498.1249, found 498.1240.

(*Z*)-3-(5-((9-Oxo-7-phenyl-5*H*-benzo[*h*]thiazolo[2,3-*b*]quinazolin-10(6*H*,7*H*,9*H*)-ylidene)methyl)furan-2-yl)benzoic Acid (12a). In the same manner as described in the preparation of **1**, **12a** was prepared from **5b** and 3-(5-formylfuran-2-yl)benzoic acid. Yield: 64.5%. HPLC: 100.00%, t_R = 5.756 min. ^{1}H NMR (300 MHz, DMSO-d_6): δ 8.38 (s, 1H), 7.93−7.83 (m, 3H), 7.54−7.49 (m, 2H), 7.40−7.12 (m, 10H), 5.84 (s, 1H), 2.84−2.73 (m, 1H), 2.67−2.57 (m, 1H), 2.39−2.28 (m, 1H), 1.98−1.86 (m, 1H). ESI-MS *m*/*z* 529 [M − H]$^-$. HRMS (EI) *m*/*z* calcd for $C_{32}H_{22}N_2O_4S$ [M$^+$] 530.1300, found 530.1308.

(*Z*)-3-(5-((7-(2-Fluorophenyl)-9-oxo-5*H*-benzo[*h*]thiazolo[2,3-*b*]-quinazolin-10(6*H*,7*H*,9*H*)-ylidene)methyl)furan-2-yl)benzoic Acid (12b). In the same manner as described in the preparation of **1**, **12b** was prepared from **5c** and 3-(5-formylfuran-2-yl)benzoic acid. Yield: 66.7%. HPLC: 100.00%, t_R = 5.432 min. ^{1}H NMR (300 MHz, DMSO-d_6): δ 8.38 (s, 1H), 7.93−7.84 (m, 3H), 7.54−7.42 (m, 4H), 7.28−7.13 (m, 7H), 5.89 (s, 1H), 2.79−2.61 (m, 2H), 2.35−2.30 (m, 1H), 1.95−1.91 (m, 1H). ESI-MS *m*/*z* 547

$[M - H]^-$. HRMS (EI) m/z calcd for $C_{32}H_{21}FN_2O_4S$ $[M^+]$ 548.1206, found 548.1213.

(*Z*)-3-(5-((7-(3-Fluorophenyl)-9-oxo-5*H*-benzo[*h*]thiazolo[2,3-*b*]-quinazolin-10(6*H*,7*H*,9*H*)-ylidene)methyl)furan-2-yl)benzoic Acid (12c). In the same manner as described in the preparation of **1**, **12c** was prepared from **5d** and 3-(5-formylfuran-2-yl)benzoic acid. Yield: 70.7%. HPLC: 100.00%, t_R = 4.974 min. ^{1}H NMR (300 MHz, DMSO-d_6): δ 8.38 (s, 1H), 7.93−7.84 (m, 3H), 7.64−7.29 (m, 3H), 7.28−7.13 (m, 8H), 5.90 (s, 1H), 2.82−2.73 (m, 1H), 2.69−2.59 (m, 1H), 2.40−2.30 (m, 1H), 1.99−1.88 (m, 1H). ESI-MS m/z 547 $[M - H]^-$. HRMS (EI) m/z calcd for $C_{32}H_{21}FN_2O_4S$ $[M^+]$ 548.1206, found 548.1200.

(*Z*)-3-(5-((7-(4-Fluorophenyl)-9-oxo-5*H*-benzo[*h*]thiazolo[2,3-*b*]-quinazolin-10(6*H*,7*H*,9*H*)-ylidene)methyl)furan-2-yl)benzoic Acid (12d). In the same manner as described in the preparation of **1**, **12d** was prepared from **5e** and 3-(5-formylfuran-2-yl)benzoic acid. Yield: 66.7%. HPLC: 100.00%, t_R = 4.593 min. ^{1}H NMR (300 MHz, DMSO-d_6): δ 8.45 (s, 1H), 8.08−7.87 (m, 6H), 7.69−7.48 (m, 5H), 7.37−7.12 (m, 3H), 6.02 (s, 1H), 2.84−2.73 (m, 1H), 2.65−2.55 (m, 1H), 2.44−2.35 (m, 1H), 1.99−1.90 (m, 1H). ESI-MS m/z 547 $[M - H]^-$. HRMS (EI) m/z calcd for $C_{32}H_{21}FN_2O_4S$ $[M^+]$ 548.1206, found 548.1215.

(*Z*)-3-(5-((7-(3-Nitrophenyl)-9-oxo-5*H*-benzo[*h*]thiazolo[2,3-*b*]-quinazolin-10(6*H*,7*H*,9*H*)-ylidene)methyl)furan-2-yl)benzoic Acid (12e). In the same manner as described in the preparation of **1**, **12e** was prepared from **5f** and 3-(5-formylfuran-2-yl)benzoic acid. Yield: 68.3%. HPLC: 97.52%, t_R = 4.978 min. ^{1}H NMR (300 MHz, DMSO-d_6): δ 8.39 (s, 1H), 8.28 (s, 1H), 8.20−8.18 (m, 1H), 7.93−7.85 (m, 4H,), 7.71−7.68 (m, 1H), 7.54−7.48 (m, 2H), 7.30−7.13 (m, 5H), 6.10 (s, 1H), 2.84−2.59 (m, 2H), 2.49−2.31 (m, 1H), 1.97−1.85 (m, 1H). ESI-MS m/z 574 $[M - H]^-$. HRMS (EI) m/z calcd for $C_{32}H_{21}N_3O_6S$ $[M^+]$ 575.1151, found 575.1163.

(*Z*)-3-(5-((7-(Naphthalen-1-yl)-9-oxo-5*H*-benzo[*h*]thiazolo[2,3-*b*]-quinazolin-10(6*H*,7*H*,9*H*)-ylidene)methyl)furan-2-yl)benzoic Acid (12f). In the same manner as described in the preparation of **1**, **12f** was prepared from **5g** and 3-(5-formylfuran-2-yl)benzoic acid. Yield: 77.2%. HPLC: 100.00%, t_R = 4.418 min. ^{1}H NMR (300 MHz, DMSO-d_6): δ 8.39 (s, 1H), 7.97−7.86 (m, 7H), 7.53−7.46 (m, 5H), 7.30−7.11 (m, 5H), 6.02 (s, 1H), 2.28−2.73 (m, 1H), 2.65−2.57 (m, 1H), 2.65−2.57 (m, 1H), 1.97−1.94 (m, 1H). ESI-MS m/z 579 $[M - H]^-$. HRMS (EI) m/z calcd for $C_{36}H_{24}N_2O_4S$ $[M^+]$ 580.1457, found 580.1449.

(*Z*)-3-(5-((7-(Furan-2-yl)-9-oxo-5*H*-benzo[*h*]thiazolo[2,3-*b*]quinazolin-10(6*H*,7*H*,9*H*)-ylidene)methyl)furan-2-yl)benzoic Acid (12g). In the same manner as described in the preparation of **1**, **12g** was prepared from **5h** and 3-(5-formylfuran-2-yl)benzoic acid. Yield: 67.2%. HPLC: 100.00%, t_R = 2.772 min. ^{1}H NMR (300 MHz, DMSO-d_6): δ 8.40 (s, 1H), 7.80−7.86 (m, 3H), 7.55−7.46 (d, 2H), 7.32−6.94 (m, 6H), 6.94−6.91 (m, 2H), 5.76 (s, 1H), 2.84−2.62 (m, 2H), 2.37−2.26 (m, 2H). ESI-MS m/z 519 $[M - H]^-$. HRMS (EI) m/z calcd for $C_{30}H_{20}N_2O_5S$ $[M^+]$ 520.1093, found 520.1101.

(*Z*)-3-(4-((7-(3-Fluorophenyl)-3-methoxy-9-oxo-5H-benzo[*h*]thiazolo-[2,3-*b*]quinazolin-10(6*H*,7H,9*H*)-ylidene)methyl)furan-2-yl)benzoic Acid (12j). In the same manner as described in the preparation of **1**, **12h** was prepared from **5p** and 3-(5-formylfuran-2-yl)benzoic acid. Yield: 55.2%. HPLC: 100.00%, t_R = 8.514 min. ^{1}H NMR (300 MHz, DMSO-d_6): δ 8.37 (s, 1H), 7.92−7.84 (m, 2H), 7.76 (m, 1H, J = 7.8 Hz), 7.55−7.38 (m, 3H), 7.26−7.13 (m, 5H), 6.83−6.74 (m, 2H), 5.86 (s, 1H), 3.74 (s, 3H), 2.77−2.70 (m, 1H), 2.64−2.58 (m, 1H), 2.35−2.29 (m, 1H), 1.91−1.89 (m, 1H). ESI-MS m/z 577 $[M - H]^-$. HRMS (EI) m/z calcd for $C_{33}H_{23}FN_2O_5S$ $[M^+]$ 578.1312, found 578.1321.

(*Z*)-3-(4-((7-(3-Methoxyphenyl)-9-oxo-5H-benzo[*h*]thiazolo[2,3-b]-quinazolin-10(6*H*,7*H*,9*H*)-ylidene)methyl)furan-2-yl)-4-methylbenzoic Acid (12i). In the same manner as described in the preparation of **1**, **12i** was prepared from **5n** and 3-(5-formylfuran-2-yl)-4-methylbenzoic acid. Yield: 66.3%. HPLC: 96.21%, t_R = 1.765 min. ^{1}H NMR (300 MHz, DMSO-d_6): δ 8.46 (s, 1H), 7.90−7.80 (m, 2H), 7.52 (s, 1H), 7.44−7.42 (m, 1H), 7.31−7.03 (m, 8H), 6.98−6.93 (m, 1H), 6.07 (s, 1H), 3.77 (s, 3H), 2.80−2.74 (m, 1H), 2.63−2.51 (m, 4H), 2.37−2.26 (m, 1H), 1.97−1.86 (m, 1H). ESI-MS m/z 573 $[M - H]^-$. HRMS (EI) m/z calcd for $C_{34}H_{26}N_2O_5S$ $[M^+]$ 574.1562, found 574.1570.

(*Z*)-3-(4-((7-(4-Methoxyphenyl)-9-oxo-5H-benzo[*h*]thiazolo[2,3-*b*]-quinazolin-10(6*H*,7*H*,9*H*)-ylidene)methyl)furan-2-yl)-4-methylbenzoic Acid (12h). In the same manner as described in the preparation of **1**, **12j** was prepared from **5o** and 3-(5-formylfuran-2-yl)-4-methylbenzoic acid. Yield: 45.7%. HPLC: 100.00%, t_R = 2.310 min. ^{1}H NMR (300 MHz, DMSO-d_6): δ 8.46 (s, 1H), 7.91−7.83 (m, 2H), 7.58 (s, 1H), 7.48−7.45 (m, 1H), 7.34−7.10 (m, 7H), 6.94−6.89 (m, 2H), 5.80 (s, 1H), 3.74 (s, 3H), 2.79−2.52 (m, 5H), 2.35−2.29 (m, 1H), 2.20−1.92 (m, 1H). ESI-MS m/z 573 $[M - H]^-$. HRMS (EI) m/z calcd for $C_{34}H_{26}N_2O_6S$ $[M^+]$ 574.1562, found 574.1574.

3-(5-((*Z*)-((*E*)-9-(3-Fluorobenzylidene)-5-(3-fluorophenyl)-3-oxo-3,5,6,7,8,9-hexahydro-2*H*-thiazolo[2,3-*b*]quinazolin-2-ylidene)methyl)-furan-2-yl)benzoic Acid (12k). In the same manner as described in the preparation of **1**, **12k** was prepared from **5l** and 3-(5-formylfuran-2-yl)benzoic acid. Yield: 64.9%. HPLC: 98.80%, t_R = 4.308 min. ^{1}H NMR (300 MHz, DMSO-d_6): δ 8.42 (s, 1H), 8.12−7.96 (m, 2H,), 7.86−7.68 (m, 2H), 7.56−7.12 (m, 10H), 5.86 (s, 1H), 2.77−2.61 (m, 2H), 2.37−2.22 (m, 2H), 1.98−1.87 (m, 2H). ESI-MS m/z 605 $[M - H]^-$. HRMS (EI) m/z calcd for $C_{35}H_{24}F_2N_2O_4S$ $[M^+]$ 606.1425, found 606.1436.

Acknowledgment. We thank Prof. Junying Yuan for the gift of the Bcl-x_L plasmid on pET32b vector and Prof. David Huang for the pGST plasmid encoding Mcl-1. The work was supported by One Hundred Talents Program of CAS, National Natural Science Foundation of China (20721003, 30870513), 863 Hi-Tech Program of China (Grants 2006AA020602 and 2006AA020402), NSFC Innovation Program for Research Group (20721003), the Ministry of Science and Technology of China (973 Program) (2007CB947100), and National Science and Technology Major Project "Key New Drug Creation and Manufacturing Program" (2009ZX09301-001, 2009ZX09501-001, and 2009ZX09501-010).

Supporting Information Available: HPLC analyses and ^{1}H NMR spectra for all target products, enantiomer separation of compound **1** and HPLC analysis of the two isomers, crystal structure of the intermediate compound **5a**−**1**, circular dichroism and BH3 peptide binding assay of Bcl-x_L mutant proteins, and cell morphology of K562 cells treated with or without compound **1**. This material is available free of charge via the Internet at http://pubs.acs.org.

References

(1) Kerr, J. F.; Winterford, C. M.; Harmon, B. V. Apoptosis. Its significance in cancer and cancer therapy. *Cancer* **1994**, *73*, 2013–2026.

(2) Del Principe, M. I.; Del Poeta, G.; Venditti, A.; Buccisano, F.; Maurillo, L.; Mazzone, C.; Bruno, A.; Neri, B.; Irno Consalvo, M.; Lo Coco, F.; Amadori, S. Apoptosis and immaturity in acute myeloid leukemia. *Hematology* **2005**, *10*, 25–34.

(3) Sattler, M.; Liang, H.; Nettesheim, D.; Meadows, R. P.; Harlan, J. E.; Eberstadt, M.; Yoon, H. S.; Shuker, S. B.; Chang, B. S.; Minn, A. J.; Thompson, C. B.; Fesik, S. W. Structure of Bcl-x_L-Bak peptide complex: recognition between regulators of apoptosis. *Science* **1997**, *275*, 983–986.

(4) Wang, J. L.; Liu, D.; Zhang, Z. J.; Shan, S.; Han, X.; Srinivasula, S. M.; Croce, C. M.; Alnemri, E. S.; Huang, Z. Structure-based discovery of an organic compound that binds Bcl-2 protein and induces apoptosis of tumor cells. *Proc. Natl. Acad. Sci. U.S.A.* **2000**, *97*, 7124–7129.

(5) Degterev, A.; Lugovskoy, A.; Cardone, M.; Mulley, B.; Wagner, G.; Mitchison, T.; Yuan, J. Y. Identification of small-molecule

inhibitors of interaction between the BH3 domain and Bcl-x(L). *Nat. Cell Biol.* **2001**, *3*, 173–182.
(6) Reed, J. C.; Pellecchia, M. Apoptosis-based therapies for hematologic malignancies. *Blood* **2005**, *106*, 408–418.
(7) Zhai, D.; Jin, C.; Satterthwait, A. C.; Reed, J. C. Comparison of chemical inhibitors of antiapoptotic Bcl-2-family proteins. *Cell Death Differ.* **2006**, *13*, 1419–1421.
(8) O'Brien, S.; Kipps, T. J.; Faderl, S.; Crump, M.; Keating, M. J.; Anderson, B.; Soho, C.; Bole, J.; Turner, R.; Viallet, J.; Cheson, B. D. A phase I trial of the small molecule pan-bcl-2 family inhibitor GX15-070 administered intravenously (IV) every 3 weeks to patients with previously treated chronic lymphocytic leukemia (CLL). *Blood* **2005**, *106*, 135A–135A.
(9) Flack, M. R.; Pyle, R. G.; Mullen, N. M.; Lorenzo, B.; Wu, Y. W.; Knazek, R. A.; Nisula, B. C.; Reidenberg, M. M. Oral gossypol in the treatment of metastatic adrenal cancer. *J. Clin. Endocrinol. Metab.* **1993**, *76*, 1019–1024.
(10) Epstein, A. L.; Levy, R.; Kim, H.; Henle, W.; Henle, G.; Kaplan, H. S. Biology of human malignant-lymphomas. 4. Functional characterization of 10 diffuse histiocytic lymphoma cell lines. *Cancer* **1978**, *42*, 2379–2391.
(11) Oltersdorf, T.; Elmore, S. W.; Shoemaker, A. R.; Armstrong, R. C.; Augeri, D. J.; Belli, B. A.; Bruncko, M.; Deckwerth, T. L.; Dinges, J.; Hajduk, P. J.; Joseph, M. K.; Kitada, S.; Korsmeyer, S. J.; Kunzer, A. R.; Letai, A.; Li, C.; Mitten, M. J.; Nettesheim, D. G.; Ng, S.; Nimmer, P. M.; O'Connor, J. M.; Oleksijew, A.; Petros, A. M.; Reed, J. C.; Shen, W.; Tahir, S. K.; Thompson, C. B.; Tomaselli, K. J.; Wang, B. L.; Wendt, M. D.; Zhang, H. C.; Fesik, S. W.; Rosenberg, S. H. An inhibitor of Bcl-2 family proteins induces regression of solid tumours. *Nature* **2005**, *435*, 677–681.
(12) Green, R. J.; Frazier, R. A.; Shakesheff, K. M.; Davies, M. C.; Roberts, C. J.; Tendler, S. J. Surface plasmon resonance analysis of dynamic biological interactions with biomaterials. *Biomaterials* **2000**, *21*, 1823–1835.
(13) Trudel, S.; Li, Z. H.; Rauw, J.; Tiedemann, R. E.; Wen, X. Y.; Stewart, A. K. Preclinical studies of the pan-Bcl inhibitor obatoclax (GX015-070) in multiple myeloma. *Blood* **2007**, *109*, 5430–5438.
(14) Vogler, M.; Weber, K.; Dinsdale, D.; Schmitz, I.; Schulze-Osthoff, K.; Dyer, M. J.; Cohen, G. M. Different forms of cell death induced by putative Bcl-2 inhibitors. *Cell Death Differ.* **2009**, *16*, 1030–1039.
(15) Zamzami, N.; Marchetti, P.; Castedo, M.; Zanin, C.; Vayssiere, J. L.; Petit, P. X.; Kroemer, G. Reduction in mitochondrial potential constitutes an early irreversible step of programmed lymphocyte death in vivo. *J. Exp. Med.* **1995**, *181*, 1661–1672.
(16) Smiley, S. T.; Reers, M.; Mottola-Hartshorn, C.; Lin, M.; Chen, A.; Smith, T. W.; Steele, G. D., Jr.; Chen, L. B. Intracellular heterogeneity in mitochondrial membrane potentials revealed by a J-aggregate-forming lipophilic cation JC-1. *Proc. Natl. Acad. Sci. U.S.A.* **1991**, *88*, 3671–3675.
(17) Mohammad, R. M.; Goustin, A. S.; Aboukameel, A.; Chen, B.; Banerjee, S.; Wang, G.; Nikolovska-Coleska, Z.; Wang, S.; Al-Katib, A. Preclinical studies of TW-37, a new nonpeptidic small-molecule inhibitor of Bcl-2, in diffuse large cell lymphoma xenograft model reveal drug action on both Bcl-2 and Mcl-1. *Clin. Cancer Res.* **2007**, *13*, 2226–2235.
(18) Zhang, M.; Ling, Y.; Yang, C. Y.; Liu, H.; Wang, R.; Wu, X.; Ding, K.; Zhu, F.; Griffith, B. N.; Mohammad, R. M.; Wang, S.; Yang, D. A novel Bcl-2 small molecule inhibitor 4-(3-methoxyphenylsulfannyl)-7-nitro-benzofurazan-3-oxide (MNB)-induced apoptosis in leukemia cells. *Ann. Hematol.* **2007**, *86*, 471–481.
(19) Rothe, G.; Valet, G. Flow cytometric analysis of respiratory burst activity in phagocytes with hydroethidine and 2′,7′-dichlorofluorescin. *J. Leukocyte Biol.* **1990**, *47*, 440–448.
(20) An, J.; Chen, Y.; Huang, Z. Critical upstream signals of cytochrome C release induced by a novel Bcl-2 inhibitor. *J. Biol. Chem.* **2004**, *279*, 19133–19140.
(21) Tsujimoto, Y.; Cossman, J.; Jaffe, E.; Croce, C. M. Involvement of the bcl-2 gene in human follicular lymphoma. *Science* **1985**, *228*, 1440–1443.
(22) Minn, A. J.; Rudin, C. M.; Boise, L. H.; Thompson, C. B. Expression of Bcl-x_L can confer a multidrug resistance phenotype. *Blood* **1995**, *86*, 1903–1910.
(23) Perego, P.; Righetti, S. C.; Supino, R.; Delia, D.; Caserini, C.; Carenini, N.; Bedogne, B.; Broome, E.; Krajewski, S.; Reed, J. C.; Zunino, F. Role of apoptosis and apoptosis-related proteins in the cisplatin-resistant phenotype of human tumor cell lines. *Apoptosis* **1997**, *2*, 540–548.
(24) Yoshino, T.; Shiina, H.; Urakami, S.; Kikuno, N.; Yoneda, T.; Shigeno, K.; Igawa, M. Bcl-2 expression as a predictive marker of hormone-refractory prostate cancer treated with taxane-based chemotherapy. *Clin. Cancer Res.* **2006**, *12*, 6116–6124.
(25) Reed, J. C. Bcl-2-family proteins and hematologic malignancies: history and future prospects. *Blood* **2008**, *111*, 3322–3330.
(26) Feng, Y.; Lin, Z.; Shen, X.; Chen, K.; Jiang, H.; Liu, D. Bcl-x_L forms two distinct homodimers at non-ionic detergents: implications in the dimerization of Bcl-2 family proteins. *J. Biochem.* **2008**, *143*, 243–252.